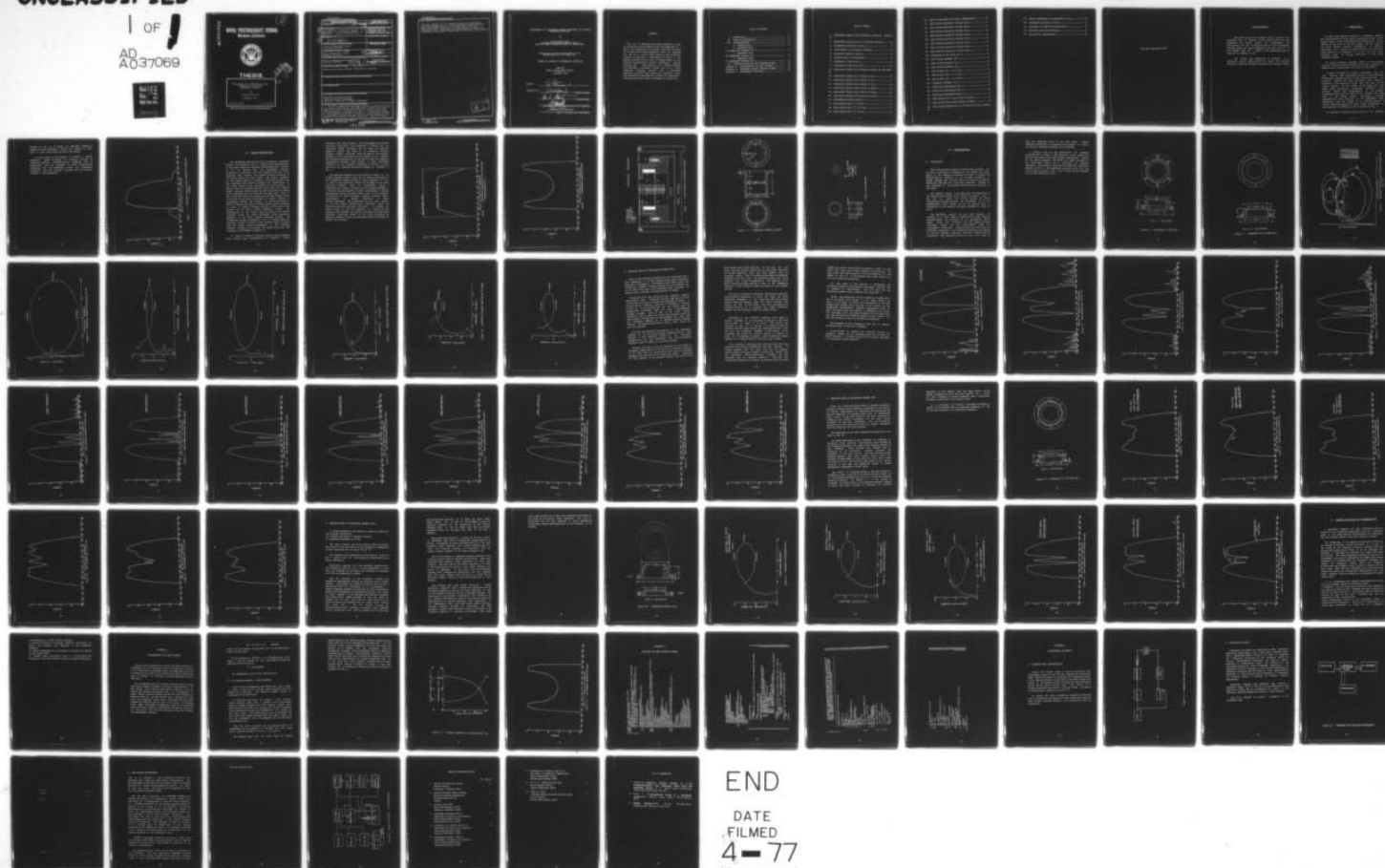AD-A037 069

NAVAL POSTGRADUATE SCHOOL MONTEREY CALIF
DEVELOPMENT OF A CONCENTRIC PISTON TRANSDUCER FOR TRACKING UNDE--ETC(U)
DEC 76   V U AUNS

F/G 17/1

UNCLASSIFIED

I OF I

AD
A037069

NL

END
DATE
FILMED
4-77

NAVAL POSTGRADUATE SCHOOL
Monterey, California

THESIS

DEVELOPMENT OF A CONCENTRIC PISTON
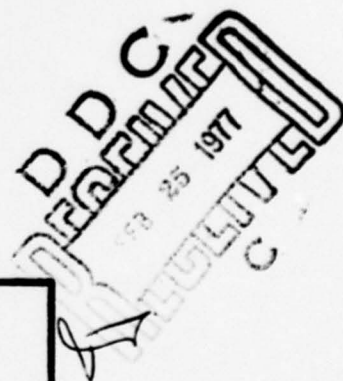TRANSDUCER FOR TRACKING
UNDERWATER VEHICLES

by

Vilnis Uldis Auns

December 1976

Thesis Advisor: O. B. Wilson

SECURITY CLASSIFICATION OF THIS PAGE (When Data Entered)

REPORT DOCUMENTATION PAGE		READ INSTRUCTIONS BEFORE COMPLETING FORM
1. REPORT NUMBER	2. GOVT ACCESSION NO.	3. RECIPIENT'S CATALOG NUMBER
4. TITLE (and Subtitle) Development of a Concentric Piston Transducer for Tracking Underwater Vehicles.		5. TYPE OF REPORT & PERIOD COVERED Master's thesis; December 1976
		6. PERFORMING ORG. REPORT NUMBER
7. AUTHOR(s) Vilnis Uldis Auns		8. CONTRACT OR GRANT NUMBER(s)
9. PERFORMING ORGANIZATION NAME AND ADDRESS Naval Postgraduate School Monterey, CA 93940		10. PROGRAM ELEMENT, PROJECT, TASK AREA & WORK UNIT NUMBERS
11. CONTROLLING OFFICE NAME AND ADDRESS Naval Postgraduate School Monterey, CA 93940		12. REPORT DATE December 1975
		13. NUMBER OF PAGES 86
14. MONITORING AGENCY NAME & ADDRESS(if different from Controlling Office) Naval Postgraduate School Monterey, CA 93940 86p.		15. SECURITY CLASS. (of this report) UNCLASSIFIED
		15a. DECLASSIFICATION/DOWNGRADING SCHEDULE

16. DISTRIBUTION STATEMENT (of this Report)

Approved for public release; distribution unlimited

17. DISTRIBUTION STATEMENT (of the abstract entered in Block 20, if different from Report)

18. SUPPLEMENTARY NOTES

19. KEY WORDS (Continue on reverse side if necessary and identify by block number)

Amplitude and Phase Shading
Concentric Piston Transducer
Composite Piezoelectric Ceramic Transducer

20. ABSTRACT (Continue on reverse side if necessary and identify by block number)

The use of amplitude and phase shading on a pair of concentric piston radiators has been employed as a means for controlling the acoustic radiation patterns for a small flush face transducer which is intended for use as a 75 kHz sound source in the underwater tracking of vehicles. A description is given of the design, construction and tests of several models of the composite piezoelectric ceramic transducer. Results indicate

DD FORM 1473 EDITION OF 1 NOV 65 IS OBSOLETE
1 JAN 73
(Page 1) S/N 0102-014-6601 |

251 450

that this appears to be a feasible method for achieving a
principal design goal of a broad beamwidth radiation pattern
with a pronounced reduction in source level along the
transducer axis. Some additional development is needed for
achieving a configuration which might be optimum for production.

DEVELOPMENT OF A CONCENTRIC PISTON TRANSDUCER FOR TRACKING
UNDERWATER VEHICLES

by

Vilnis Uldis Auns
Lieutenant-Commander,Canadian Forces
B.S.E.E. Royal Military College of Canada,1965.

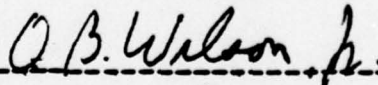Submitted in partial fulfillment of the
requirements for the degree of

MASTER OF SCIENCE IN ENGINEERING ACOUSTICS

from the
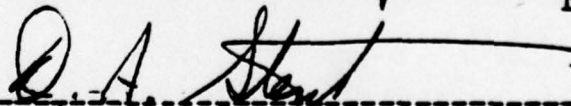NAVAL POSTGRADUATE SCHOOL
December 1976

Author: _____

Approved by: _____O.B.Wilson,Jr._____
                                    Thesis Advisor

_____
                                    Second Reader

_____
Chairman,Department of Physics and Chemistry

_____
                      Dean of Science and Engineering

3

ABSTRACT

The use of amplitude and phase shading on a pair of concentric piston radiators has been employed as a means for controlling the acoustic radiation patterns for a small flush face transducer which is intended for use as a 75 kHz sound source in the underwater tracking of vehicles. A description is given of the design, construction and tests of several models of the composite piezoelectric ceramic transducer. Results indicate that this appears to be a feasible method for achieving a principal design goal of a broad beamwidth radiation pattern with a pronounced reduction in source level along the transducer axis. Some additional developement is needed for achieving a configuration which might be optimum for production.

TABLE OF CONTENTS

LIST OF FIGURES

(This page intentionally blank)

ACKNOWLEDGEMENTS

The author, just as the numerous thesis students who preceeded him ,is indebted to Mr. Robert Moeller for his assistance and advice during the construction and modification of the transducers used for this development work. The prompt but highly dependable work that came out of his machine shop was a credit to his professionalism and should be an example to all.

The advice and experience of Professor O. B. Wilson, the thesis advisor, gave the author the required judicious push when personal abilities were becoming taxed.

I. INTRODUCTION

For many years acoustic tracking of underwater weapons
has been achieved by using small transducers mounted on the
weapon itself. Their transmissions are monitored by arrays
mounted on the bottom of the test ranges. The test range of
the Naval Torpedo Station (NAVTORPSTA) at Keyport,
Washington has a matrix of arrays mounted on the sea floor
which operate at a frequency of 75 Khz and each array
provides range and bearing information to the shore
computing station.

To ensure accurate tracking whilst on the tracking
range,the radiation pattern should be of such character to
insonify some minimum number of arrays on the bottom.

A variety of designs of pinger transducers have been
used. Pop-out type transducers utilize a small spherical
piezoelectric ceramic element as the radiating source. Its
radiation pattern has been considered quite adequate.
However,it is not physically flush with the body of the
target vehicle. If the target vehicle should be a high
speed modern torpedo,the protruding transducer would
severely affect the hydrodynamics of the torpedo.
Transducers flush with the body of the torpedo have been
used in the recent years. According to informal
communications from personnel at the NAVTORPSTA their
operational life has proven to be relatively short. A
typical radiation pattern for these flush transducers has
been provided by NAVTORPSTA and is attached as Fig. 1.

An approach to achieving good control of the radiation

11

pattern is the use of phase and amplitude shading of concentric piston radiators. These were studied by Shaw (Ref. 1) and a scale model was built and tested.

It is the intent of this thesis to develope a phased concentric piston transducer for acoustic tracking of underwater vehicles. Specifically,the transducer will be constructed with the objective of being operationally compatible with the underwater ranges and physically compatible with the extender sections used with exercise torpedos at the NAVTORPSTA .
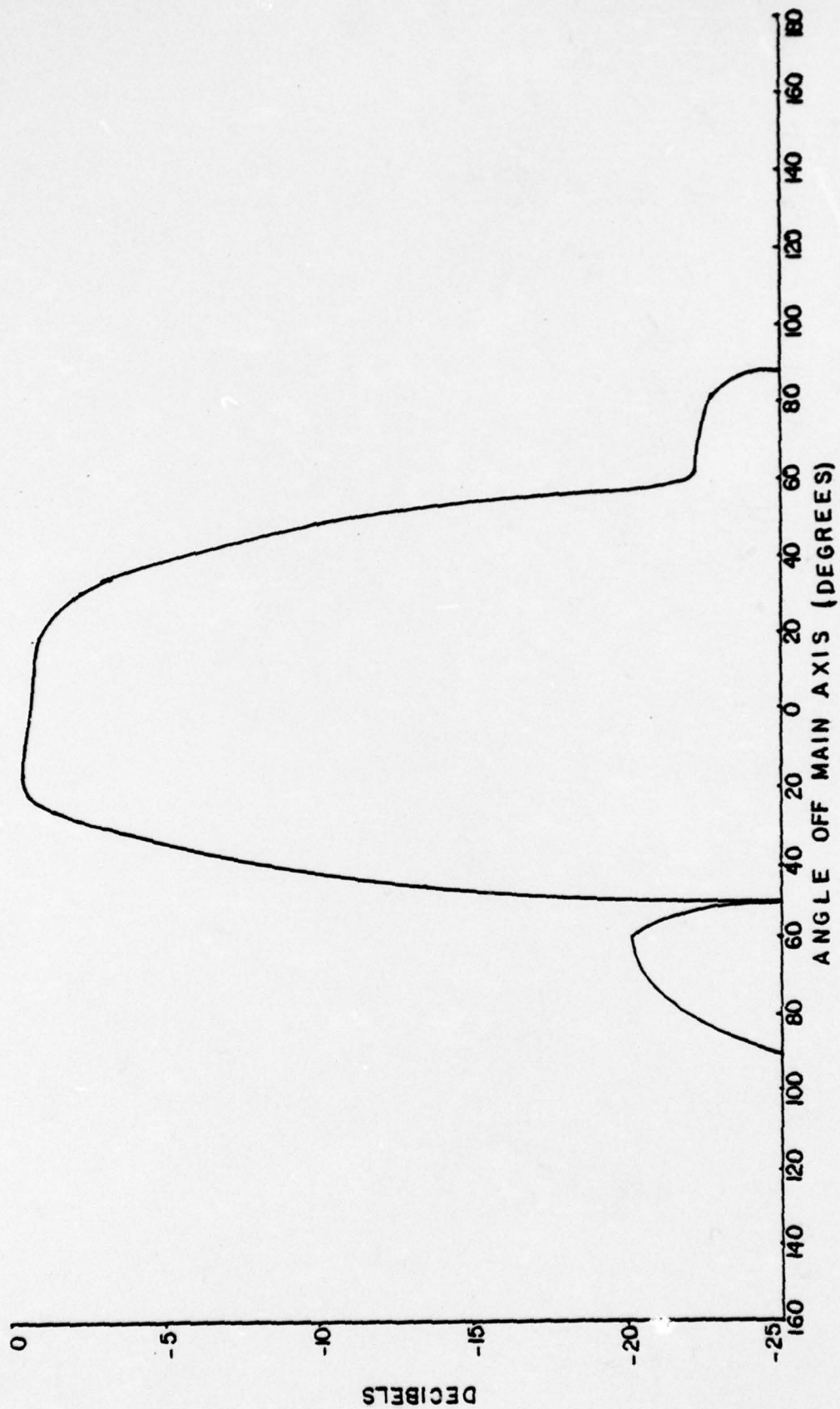
Figure 1 – NAVTORPSTA TYPICAL FLUSH TRANSDUCER RADIATION
PATTERN

ANGLE OFF MAIN AXIS (DEGREES)

DECIBELS

13

II. DESIGN CONSIDERATIONS

The NAVTORPSTA specification for the required radiation pattern is attached as Fig. 2. However,from considerations of the actual needs for intensity distribution,this pattern is not an optimum one. The transducer's physical orientation is such that their main physical axis and their radiation axis coincide and project from the underside of the vehicle toward the ocean bottom. The design objective of this thesis shall be to achieve a radiation pattern from the transducer which tends to optimize the distribution of the sound energy to the array matrix on the sea floor. To achieve this the radiation pattern should have the minimum signal strength directly down the main axis,with the source level increasing with the angle off the main axis. This is due to the fact that at any depth the maximum acoustic range to an array is the slant range when the target vehicle is equidistant between the arrays. At and above angles of about 70 degrees the signal strength should rapidly decrease in order to reduce acoustic coupling to the frame of the vehicle and to reduce surface reflected sound. The re-radiation of the pulses from the frame or the surface scattered pulses can cause additional range processing problems in the shore station computing system. The recommended pattern of Appendix A (Fig. 3) would enable the receiving arrays to receive a more constant level of signal from the target vehicle,irrespective of the vehicles physical position on the range. The justification for this statement is developed in Appendix A.

In order to achieve a radiation pattern which resembles this optimum one,a configuration of concentric piston

radiators has been utilized. The development here follows the work of LCDR Shaw. Shaw (Reference 1) showed how two concentric piston radiators can be phase and amplitude shaded to control the shape of the radiation pattern. Computer studies indicated that the phase of the relative movement of the radiating faces was optimal at 180 degrees. The radiating surfaces are at one end of a pair of composite longitudinal vibrators which operate at half wavelength resonance at the intended frequency of 75 Khz. A cross section of the intended transducer assembly is attached as Fig. 4.

The physical dimensions of the mounting flange on the torpedo extender section restricts the outside dimensions of the transducer assembly housing to those displayed on Fig. 5. This in turn physically limits the diameter of the outer radiating cylinder. Based on computations using a modification of Shaw's radiation pattern program (Appendix B) and upon the availability of stock piezoelectric ceramic elements, the ceramic elements shown in Fig. 6 were selected. The material is a lead zirconate titanate (Channel 5800), manufactured by Channel Industries of Santa Barbara, California. The polarization on the outer ceramic is in the radial direction. The cylindrical discs are polarized along the thickness direction. By joining the ground leads of the two radiators and joining the two positive leads together and driving them with the same power amplifier source, the effect of the above transverse and parallel coupling is that the radiating faces are driven 180 degrees out of phase.

15

IDEAL PATTERN 100db

Minimum 93db ref 1μbar 1yard

ANGLE OFF MAIN AXIS (DEGREES)

DECIBELS
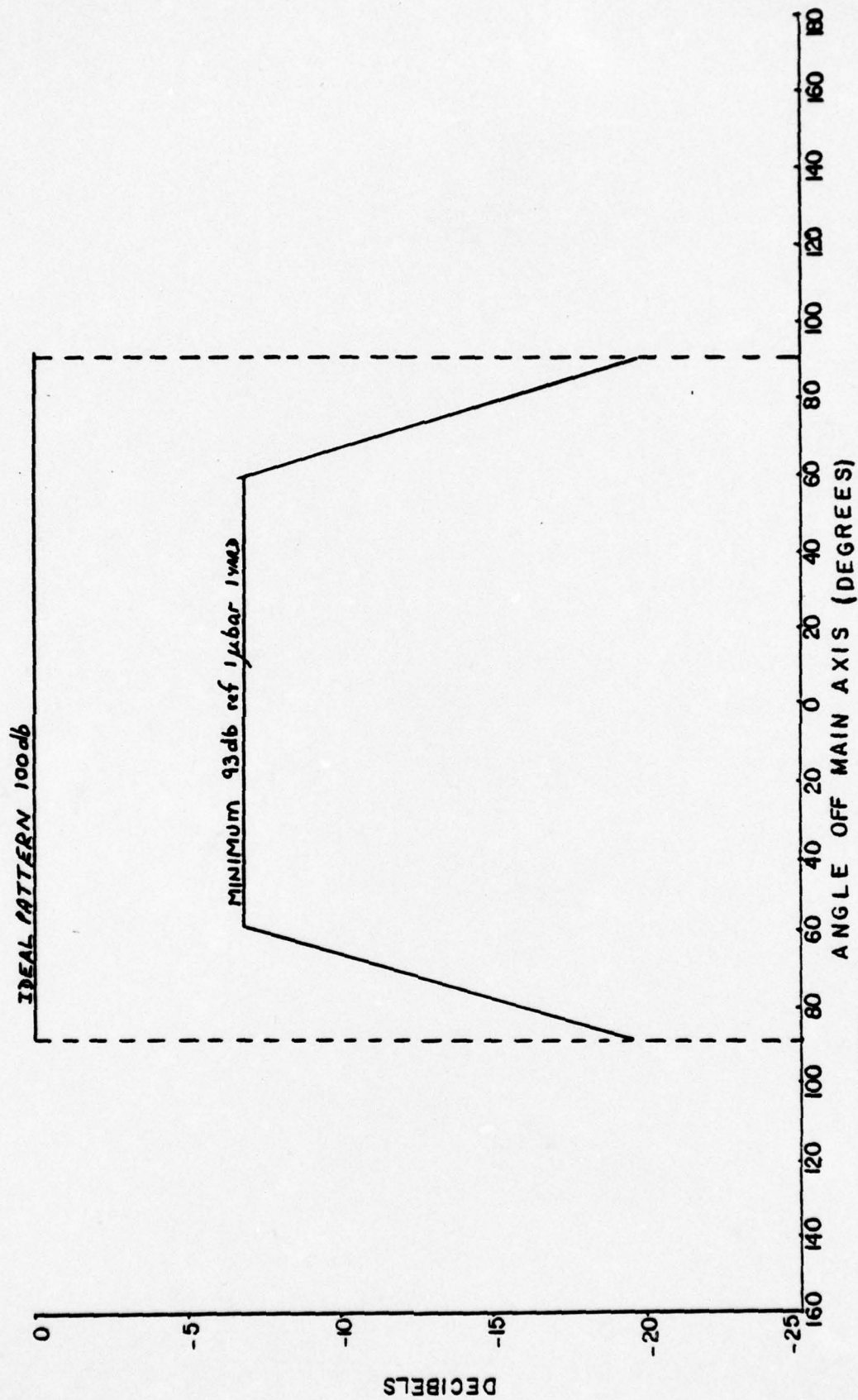
Figure 2 – NAVTORPSTA SPECIFICATION FOR RADIATION
PATTERN (REFERENCE 3)

16

ANGLE OFF MAIN AXIS (DEGREES)
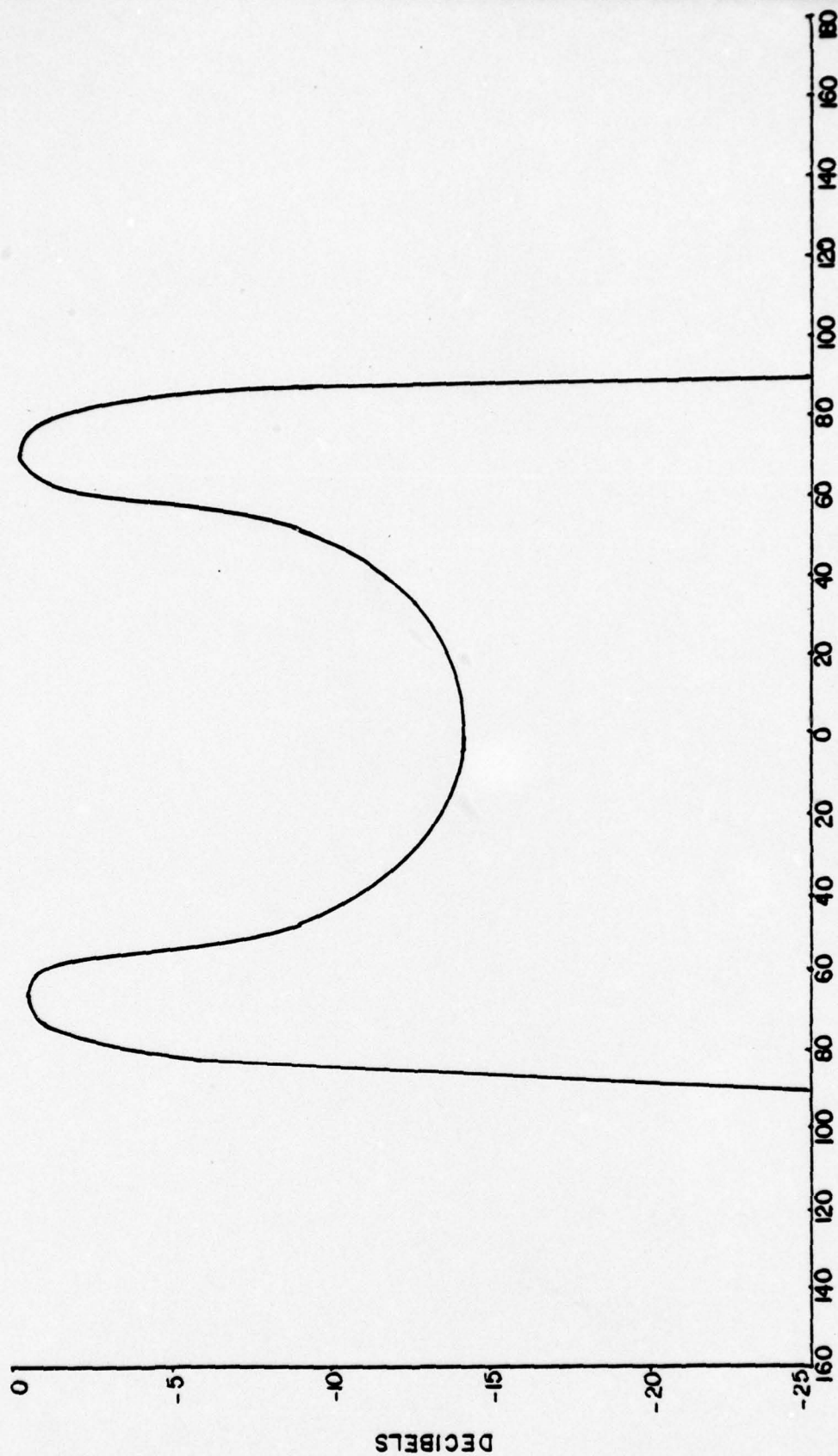
Figure 3 - RECOMMENDED RADIATION PATTERN

DECIBELS

17
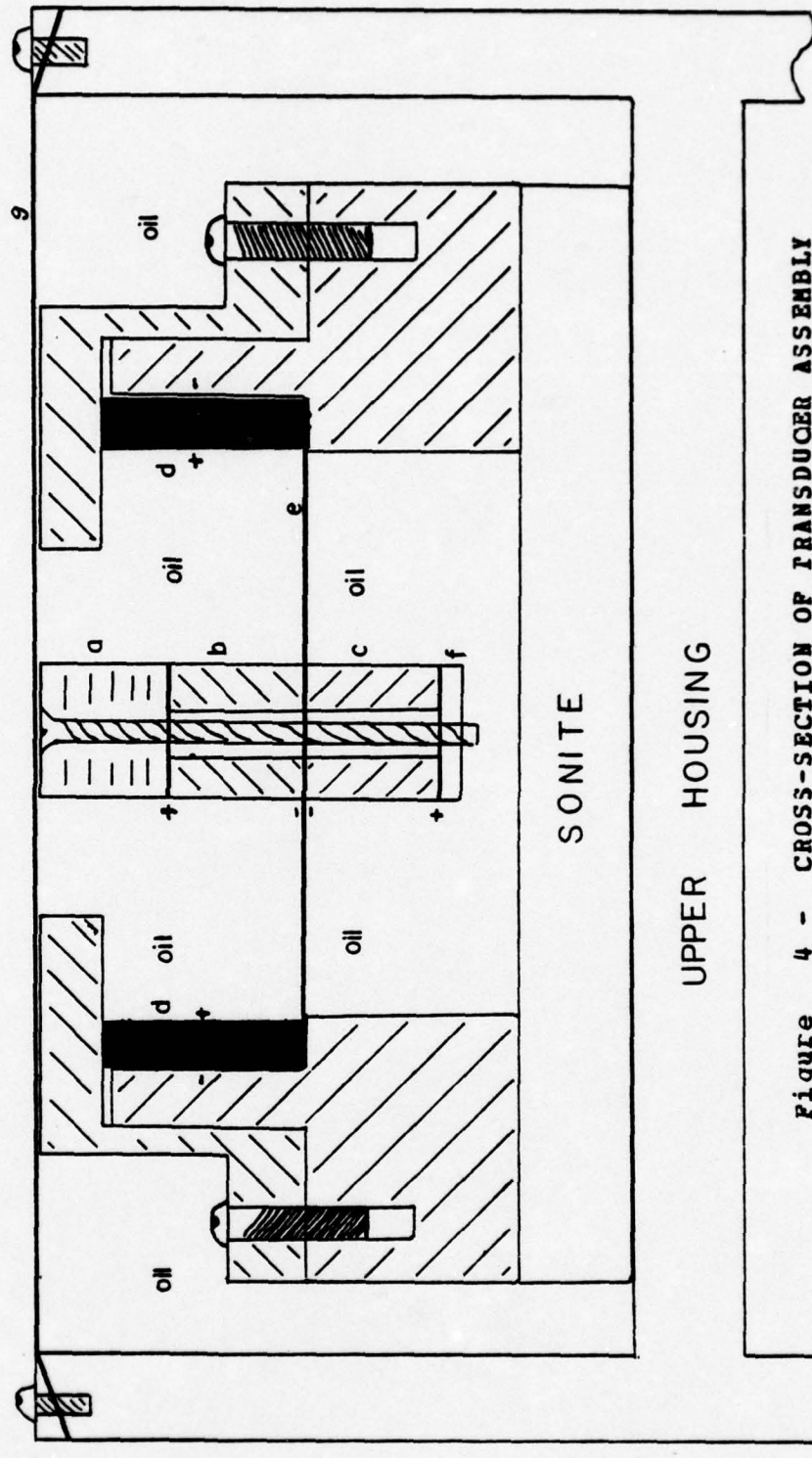
Figure 4 – CROSS-SECTION OF TRANSDUCER ASSEMBLY
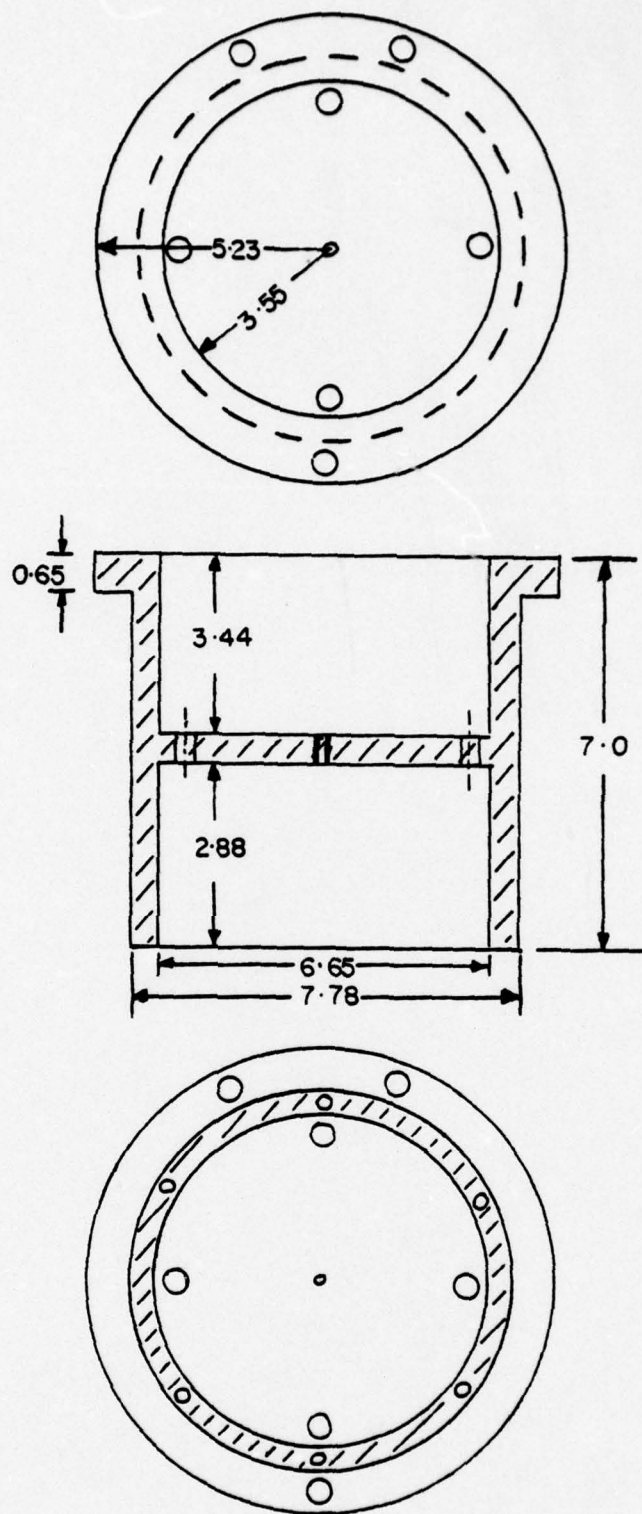
Figure   5 -   TRANSDUCER ASSEMBLY HOUSING

UNITS IN CENTIMETERS

.635

.635

1.9

.63

.318

3.175

2.54

1.9
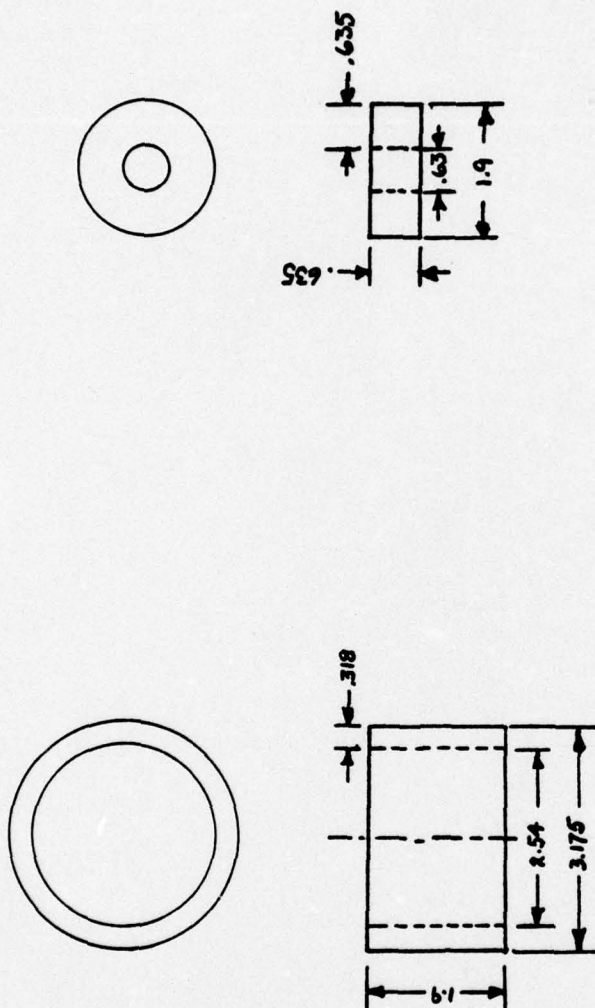
Figure 6 – CERAMICS USED IN CONSTRUCTION

III. EXPERIMENTATION

A. CONSTRUCTION

There were several practical construction problems. One was that of arriving at dimensions of the ceramic and metal parts of the composite resonators in order to achieve the desired mode of vibration at the desired frequency. A second problem was to mount the two resonators to provide mechanical stability with acoustical isolation. Changes in the solutions to one problem interacted with solutions to the other.

The initial design of the enclosure and dimensions of the radiating face of the outer piston are shown in Fig. 7 and Fig. 8. These two pieces enclose the outer piezoelectric ceramic cylinder and pre-stress it by the compressional force caused by the six joining bolts. A crossection of the finished transducer assembly is seen in Fig 4.

The mechanical support for the inner vibrator is provided by a thin sheet of steel (8 mils thick) which is clamped between the elements at the approximate middle point. Since the vibrators are not symmetrical, the attachment points are not displacement nodes for longitudinal vibrations. However, this thin sheet metal is reasonably compliant in the transverse direction and appears to provide adequate vibration isolation between the two resonators. This assymetry was due in part to the need to

21

have the radiating faces in the same plane. Careful repeated adjustments of dimensions were required to obtain the desired resonance frequency and pre-stress.

A critical part of the construction and assembly procedure was to achieve a good mechanical joint between the Top and Base pieces along with proper compressional loading of the ceramic element. The effect of a small clearance at the joint,which results in a multitude of spurious mechanical resonances,is shown in the electrical admittance diagram of Fig. 9. The admittance diagrams in the air and in the water as shown in Fig. 10 to 14 were finally achieved with a good mechanical joint.
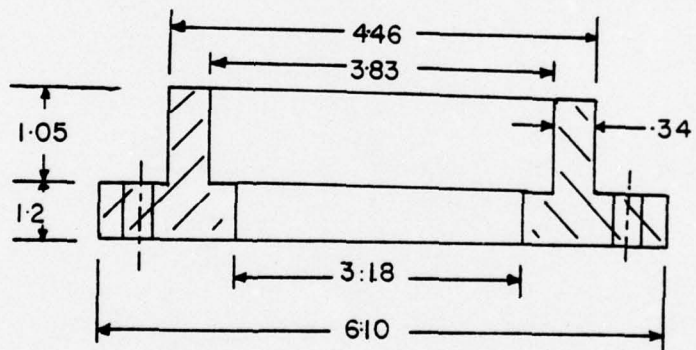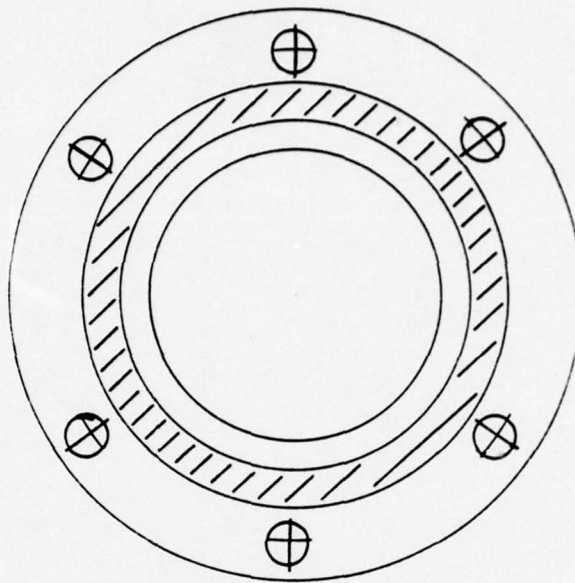
UNITS = CENTIMETRS

Figure 3 - DIMENSIONS OF BASE MOD 0

23
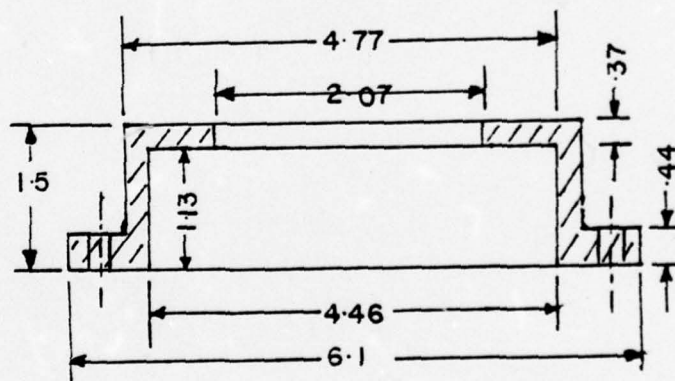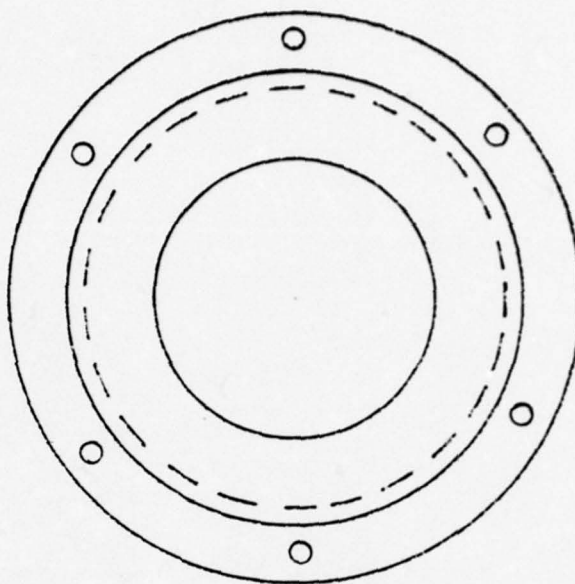
UNITS IN CENTIMETERS

Figure 8 - DIMENSIONS OF TOP PIECE MOD 0

① 98.5 Khz
② 95.1 Khz
③ 86.5 Khz
④ 82.2 Khz
⑤ 76.6 Khz
⑥ 57.5 Khz
⑦ 46.3 Khz
⑧ 44.8 Khz

CONDUCTANCE

SUSCEPTANCE
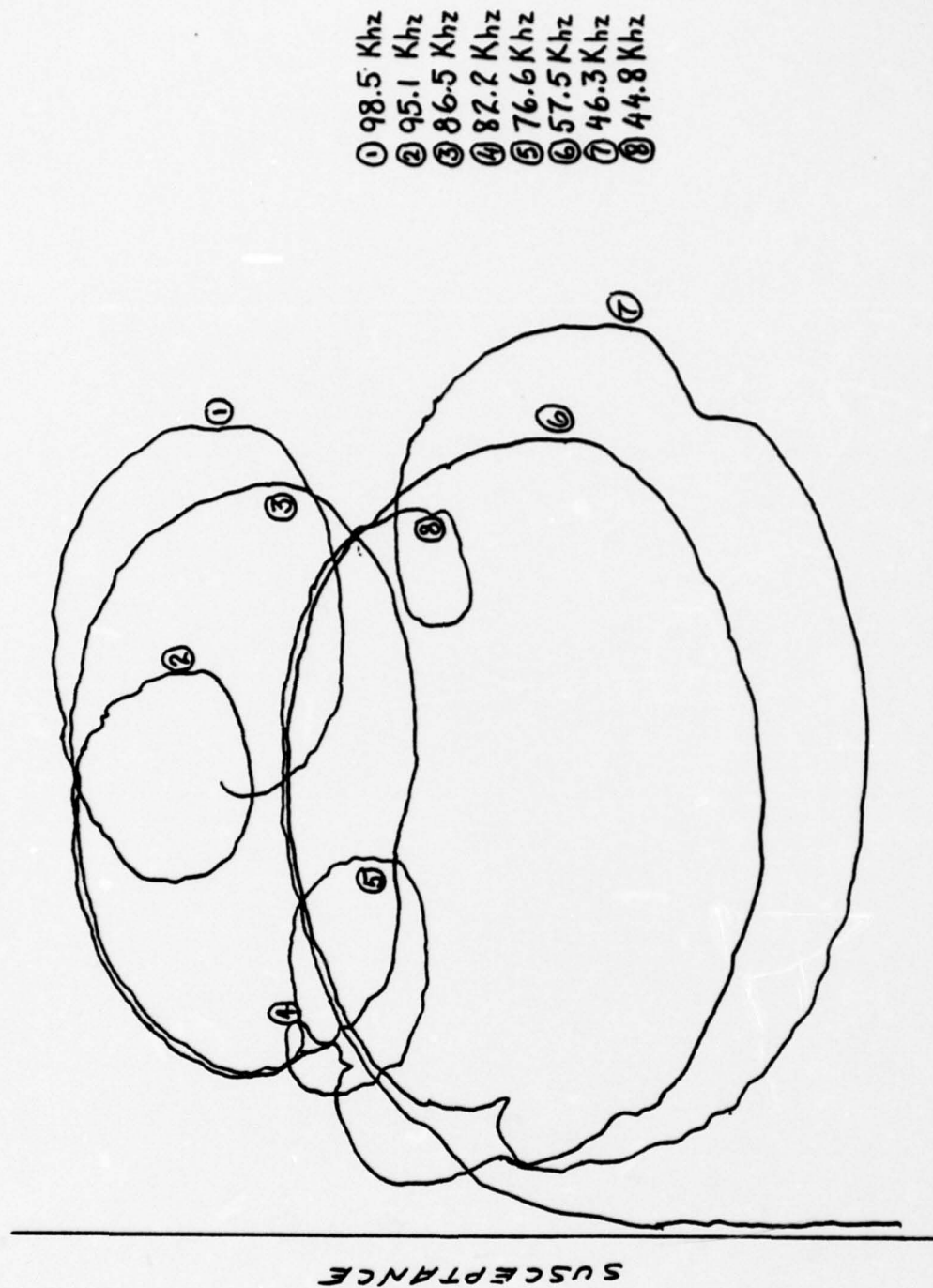
Figure 9 – ADMITTANCE DIAGRAM WITH CLEARANCE BETWEEN TOP
AND BASE

25
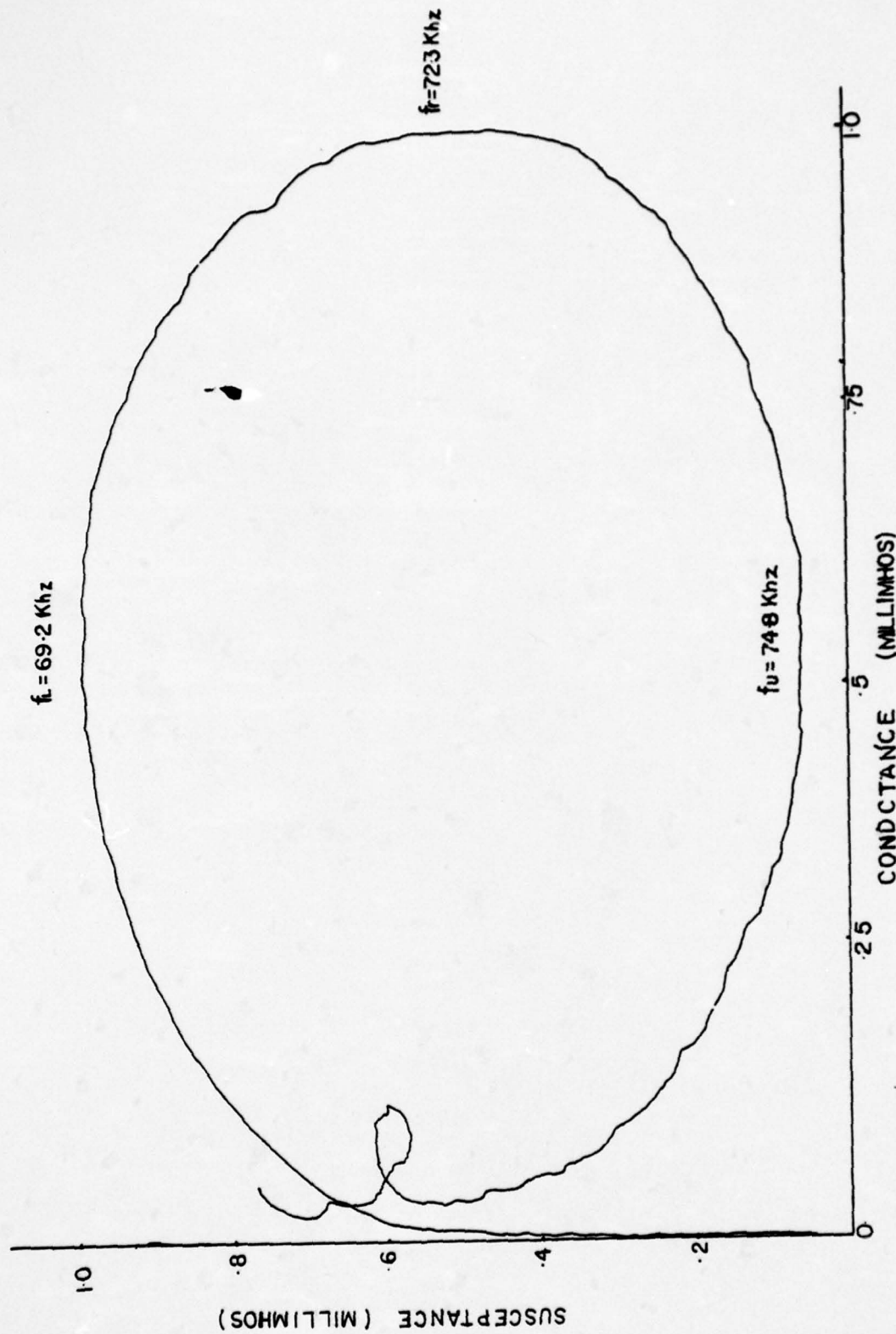
Figure 10 – ADMITTANCE DIAGRAM INNER PISTON IN AIR
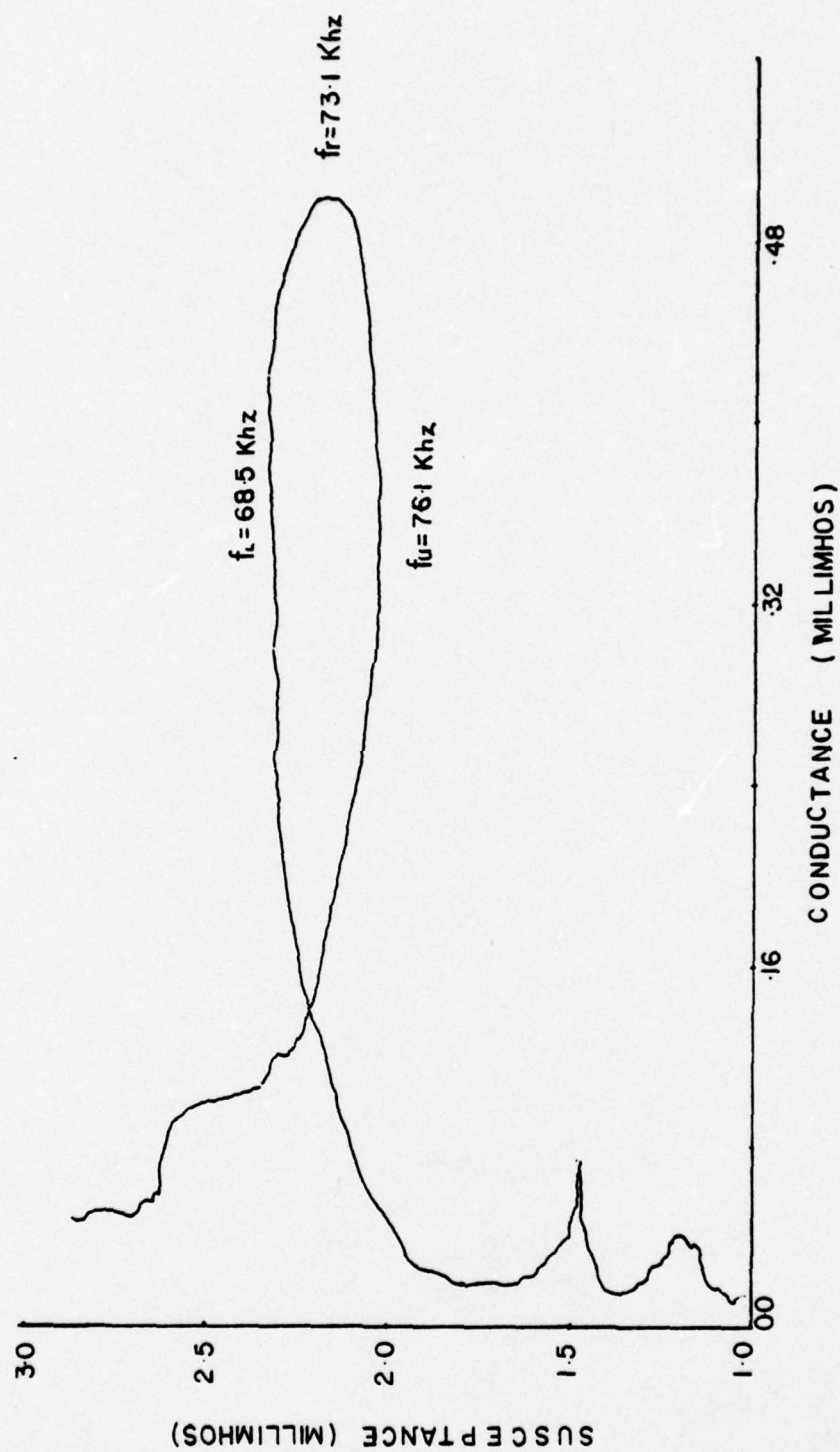
Figure 11 - ADMITTANCE DIAGRAM OUTER PISTON IN AIR

f$_L$=68·5 Khz

f$_r$=73·1 Khz

f$_u$=76·1 Khz

CONDUCTANCE (MILLIMHOS)

SUSCEPTANCE (MILLIMHOS)

27
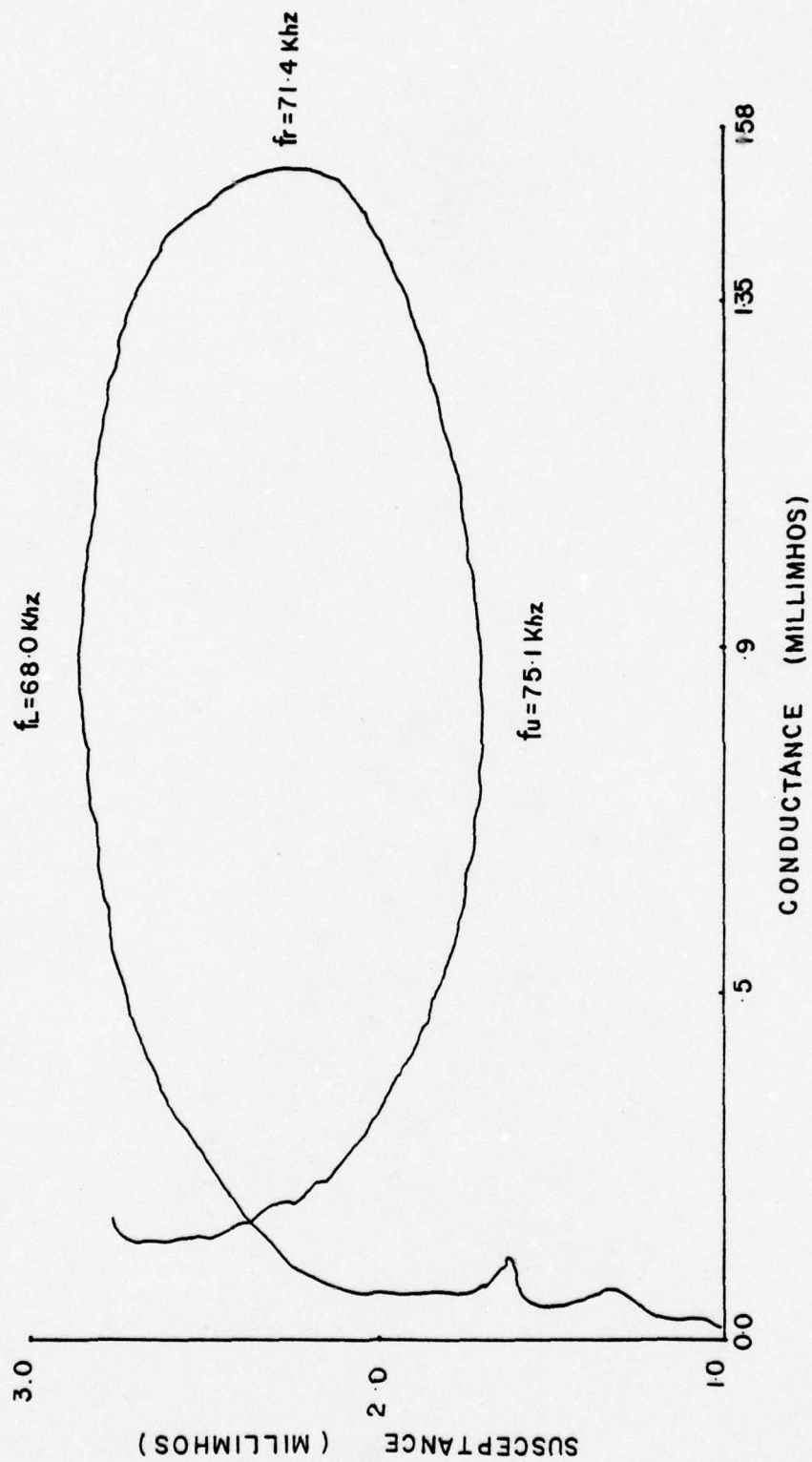
Figure 12 - ADMITTANCE DIAGRAM BOTH PISTONS IN AIR

28
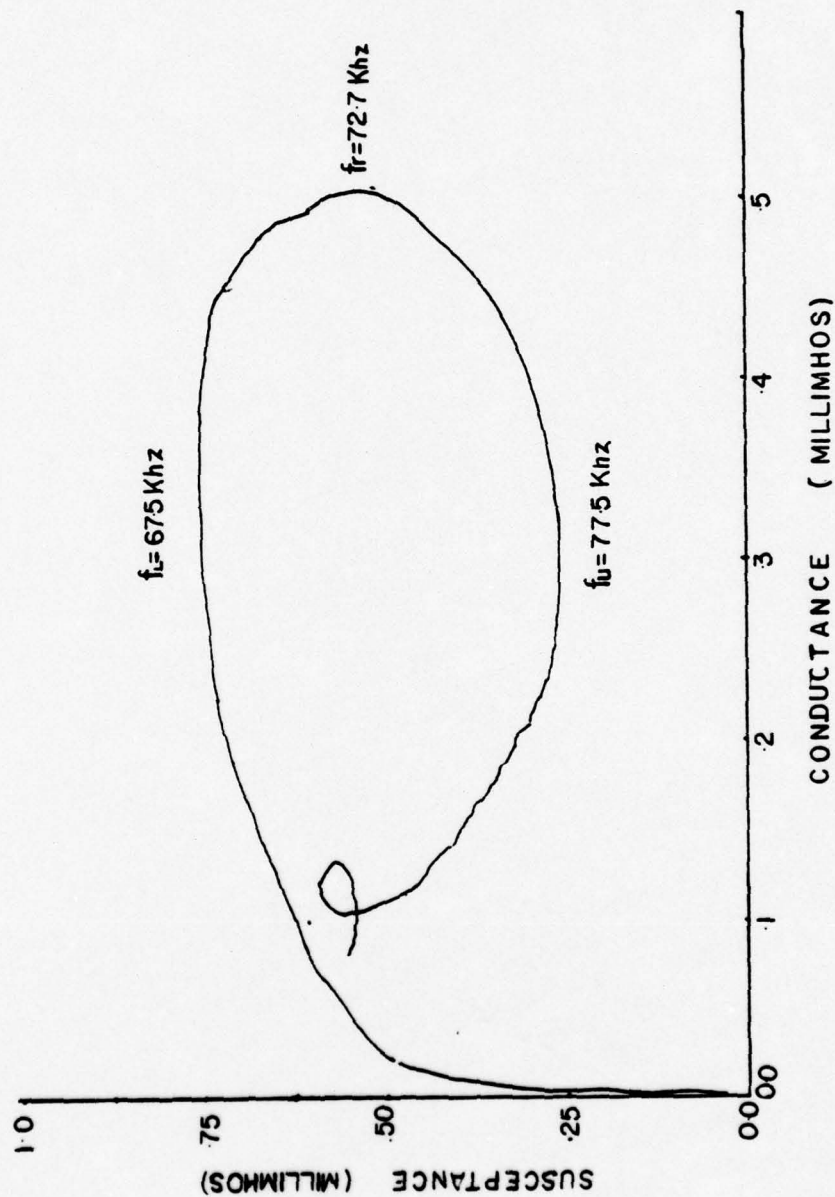
Figure 13 - ADMITTANCE DIAGRAM INNER PISTON IN WATER

fᵢ=69·4 Khz

fr=72·9 Khz

fu=75·7 Khz

SUSCEPTANCE (MILLIMHOS)

2·0

1·75

1·5

1·25

1·0

0·0 .11 .22 .33 .44

CONDUCTANCE (MILLIMHOS)
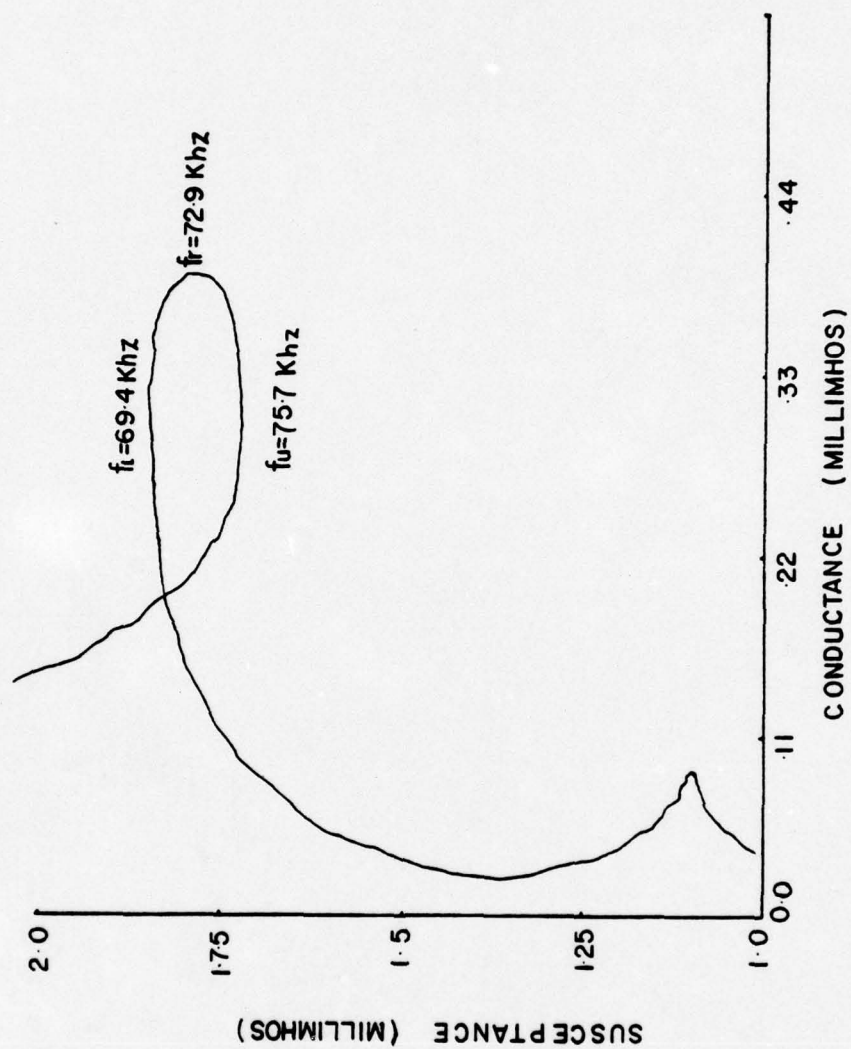
Figure 14 — ADMITTANCE DIAGRAM OUTER PISTON IN WATER

30
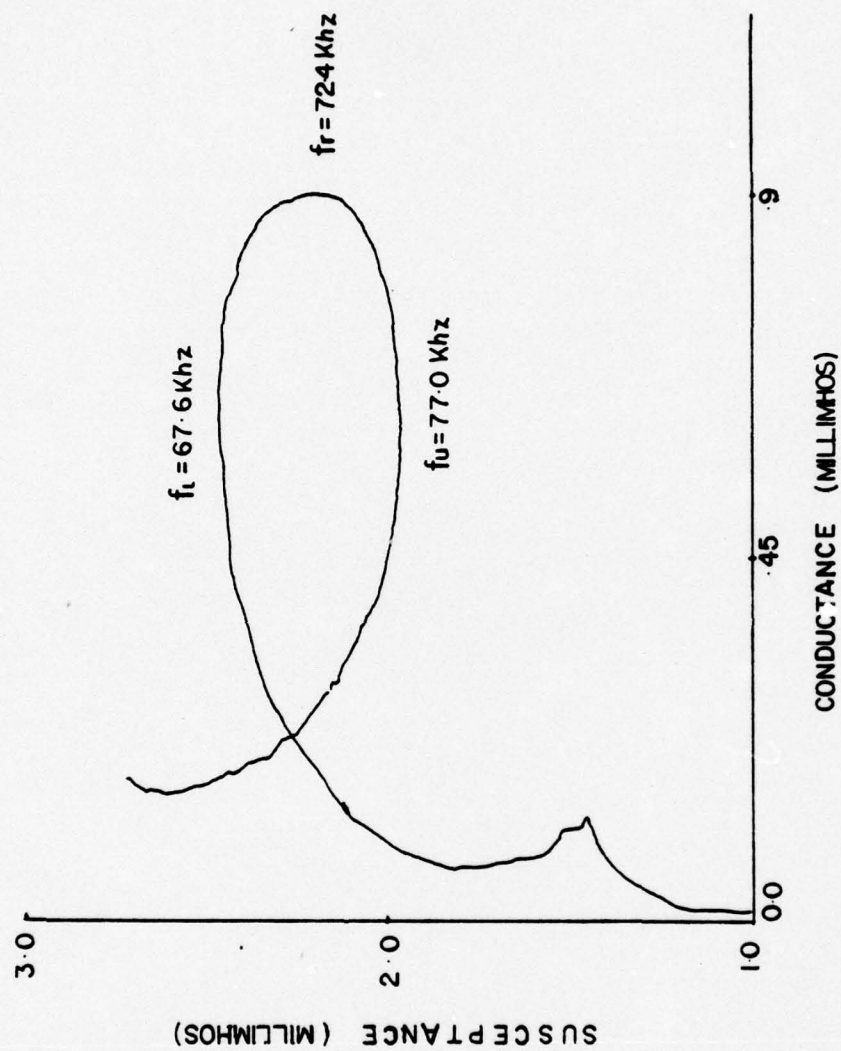
Figure 15 - ADMITTANCE DIAGRAM BOTH PISTONS IN WATER

31

B.   RADIATION TESTS OF TRANSDUCER ASSEMBLY MOD 0

Tests of the radiation patterns for the transducer Mod 0 were performed in the NPS anechoic tanks using procedures described in Appendix C. For these initial tests ,only, the cylindrical torpedo extender section was not available and so the baffle used was a plain aluminum sheet ,octogonal in shape,having a diameter of approximately 12 inches.

Parameters which were varied for the radiation pattern measurements were: frequency, relative amplitude of drive to the inner and outer radiators and magnitude of drive.   A representative recording from the x-y recorder is attached as Fig. 16. It can be seen that for the angles past 90 degrees(back radiation) there are lobes of considerable strength present. This is due to the small baffle employed.It will be seen that these back radiation lobes are significantly reduced when the measurements are done with the transducer assembly in an exercise torpedo extender section. The desired reduction in source level along the axis was achieved.

The next step entailed the mounting of the transducer assembly in the now sealed torpedo extender section. This provides a more realistic baffle for the transducer assembly,with the only difference that the longitudinal dimension would be longer in an actual torpedo.

Figures 17,18 and 19 give an indication of the effect of frequency change from 64 to 79 Khz on the radiation pattern. It is seen that at frequencies lower than the resonance frequency,the central lobe is relatively higher. Comparison of the patterns in the extender section with those in the

32

plain baffle can be done with Fig. 16 and Fig. 18. The first and most obvious effect was the significant reduction of the back radiation lobes that were present with the octogonal baffle. Also far better destructive interference occurred on the main axis. The radiation pattern was again examined over a band of frequencies. The assymetry of the lobes with the extender section is due to the assymetric location of the transducer along the length of the extender section.

The study of effects of amplitude shading were conducted using separate amplifiers to drive the inner and outer transducer elements. It was found that the most optimum pattern shape was achieved when the drive voltages were within one volt of each other. Fig. 20 is attached to be compared with Fig. 18 to indicate the slight difference between the two different kinds of voltage drives.

Recordings of the radiation patterns were taken at driving voltages of 25 volts peak to peak up to 340 volts peak to peak- in steps of 35 volts. The results are attached as Fig. 21 to Fig 28. It is apparent that the radiation pattern deteriorates with increased voltage drive and that the transducer assembly is non linear. If the transducer were linear the pattern should be similar in shape but of different strength. This nonlinearity became apparent at a voltage drive of 200 volts peak to peak.

In an attempt to determine the cause, the inner and outer radiators were driven independantly and then together. It became apparent that the outer ring was the dominant radiator,which initially seemed to counter the belief that the transverse electro-mechanical coupling was less efficient than the parallel coupling. Also,the back radiation(90 degrees and greater) was greater than the outer

33

element was driven alone, which was possibly caused by the outer ring being more closely coupled to the housing. The most likely cause was believed to be the saturation of the SONITE by the oil in the housing which would cause it to lose its decoupling properties.

At this point it was decided to disassemble the transducer, examine it for possible structural failings and to redesign for improvements. This was done and the transducer assembly which resulted was called MOD 1.

During the examination of the transducer assembly MOD 0 one of the leads to the ceramic of the inner piston was found to be loose. It could not be determined at the time whether this occured during the test or was caused by the dismantling process, which required significant force to shear the Sonite from the housing. As expected, the Sonite was saturated with oil, giving credance to the belief that the outer cylinder was directly coupled to the housing and that the Sonite had lost its decoupling properties.

This resulted in more attention to the job of sealing the Sonite prior to the MOD 1 assembly.

It was decided to improve the radiation pattern by dimension changes of the radiating faces of the inner and outer radiators. A stronger pattern at the larger angles(60 to 75 degrees) seemed desirable.

73.4 KHz

ANGLE OFF MAIN AXIS (DEGREES)

DECIBELS
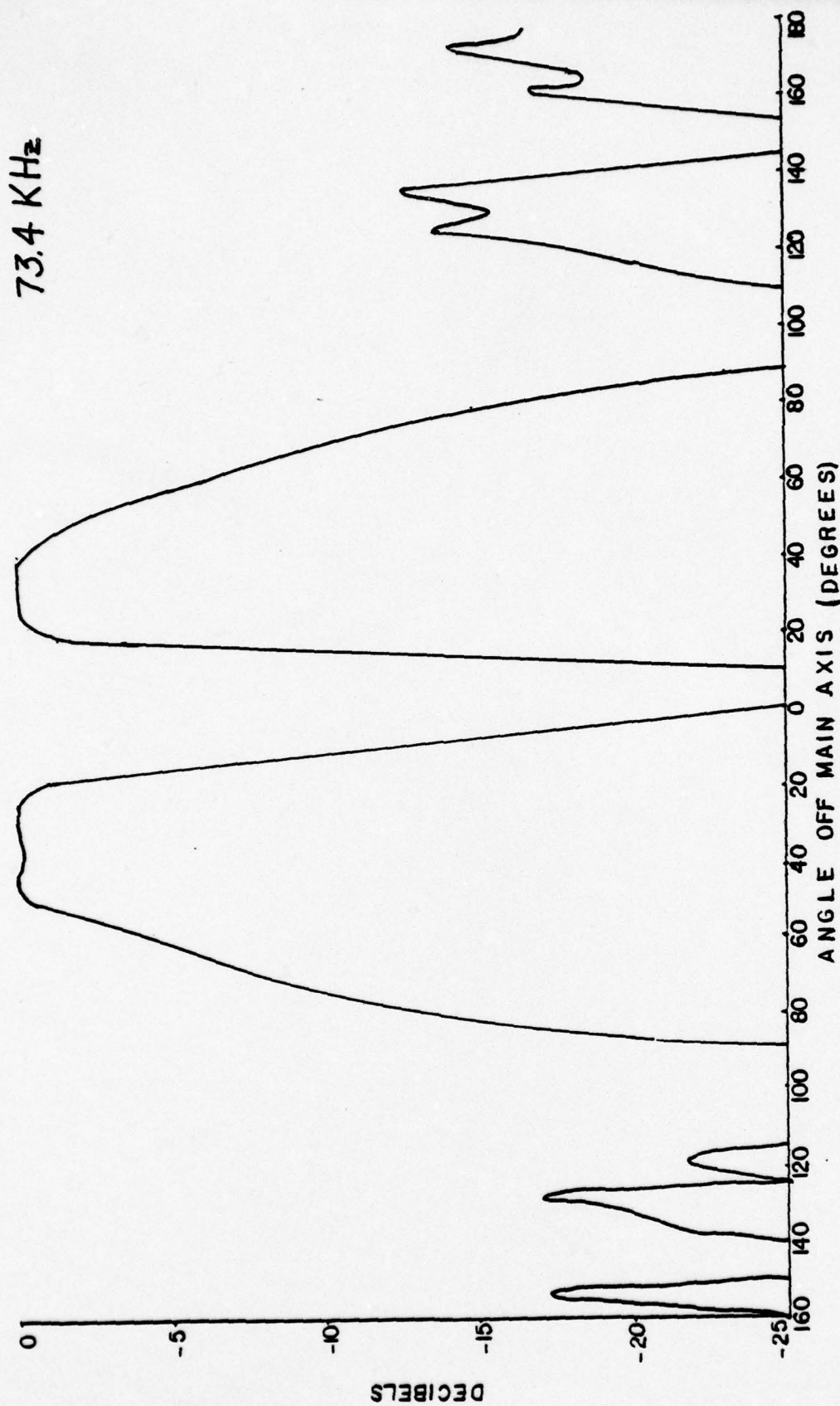
Figure 16 - REPRESENTATIVE BEAM PATTERN
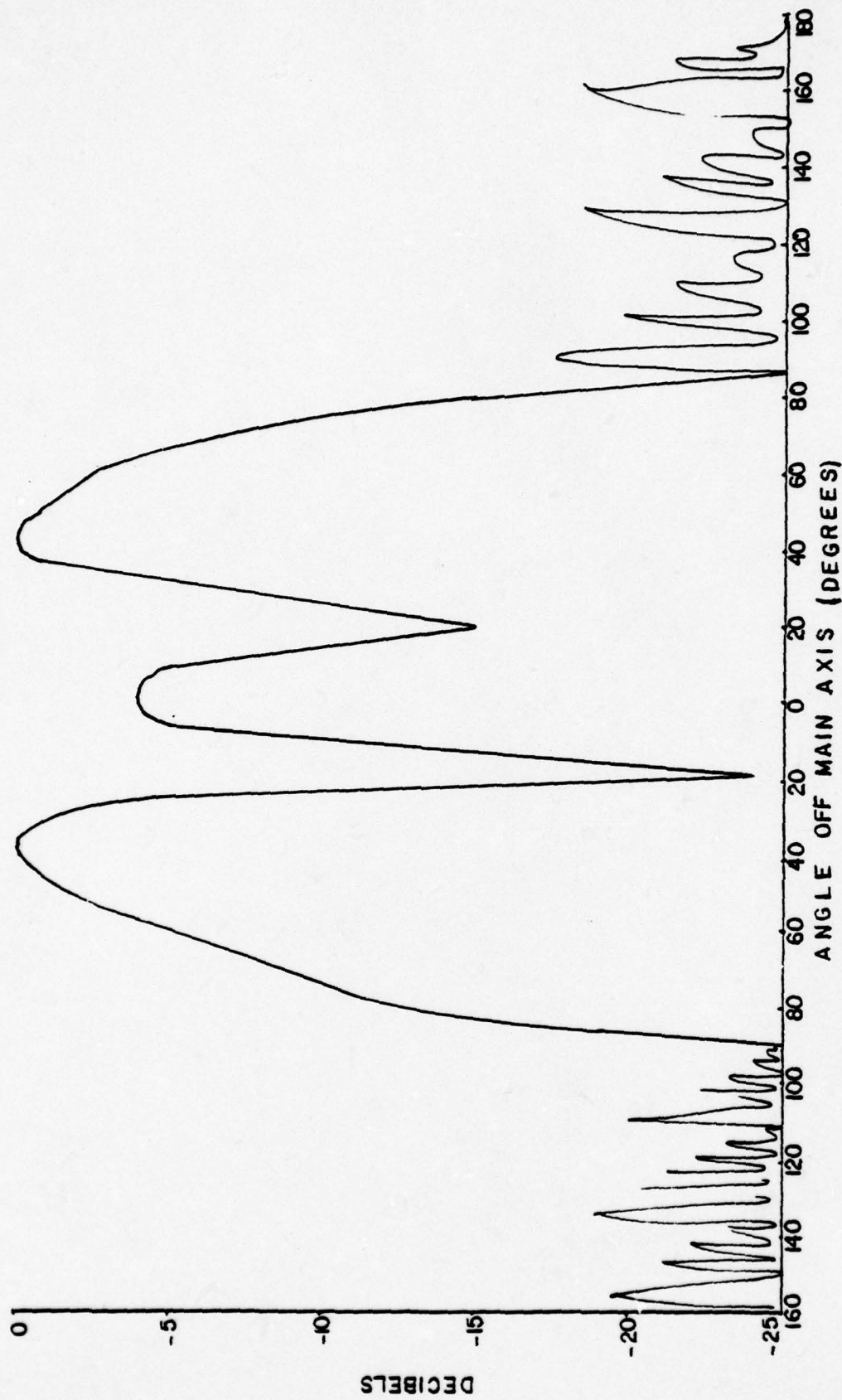
Figure 17 - BEAM PATTERN MOD 0 AT 64 KHZ

ANGLE OFF MAIN AXIS (DEGREES)
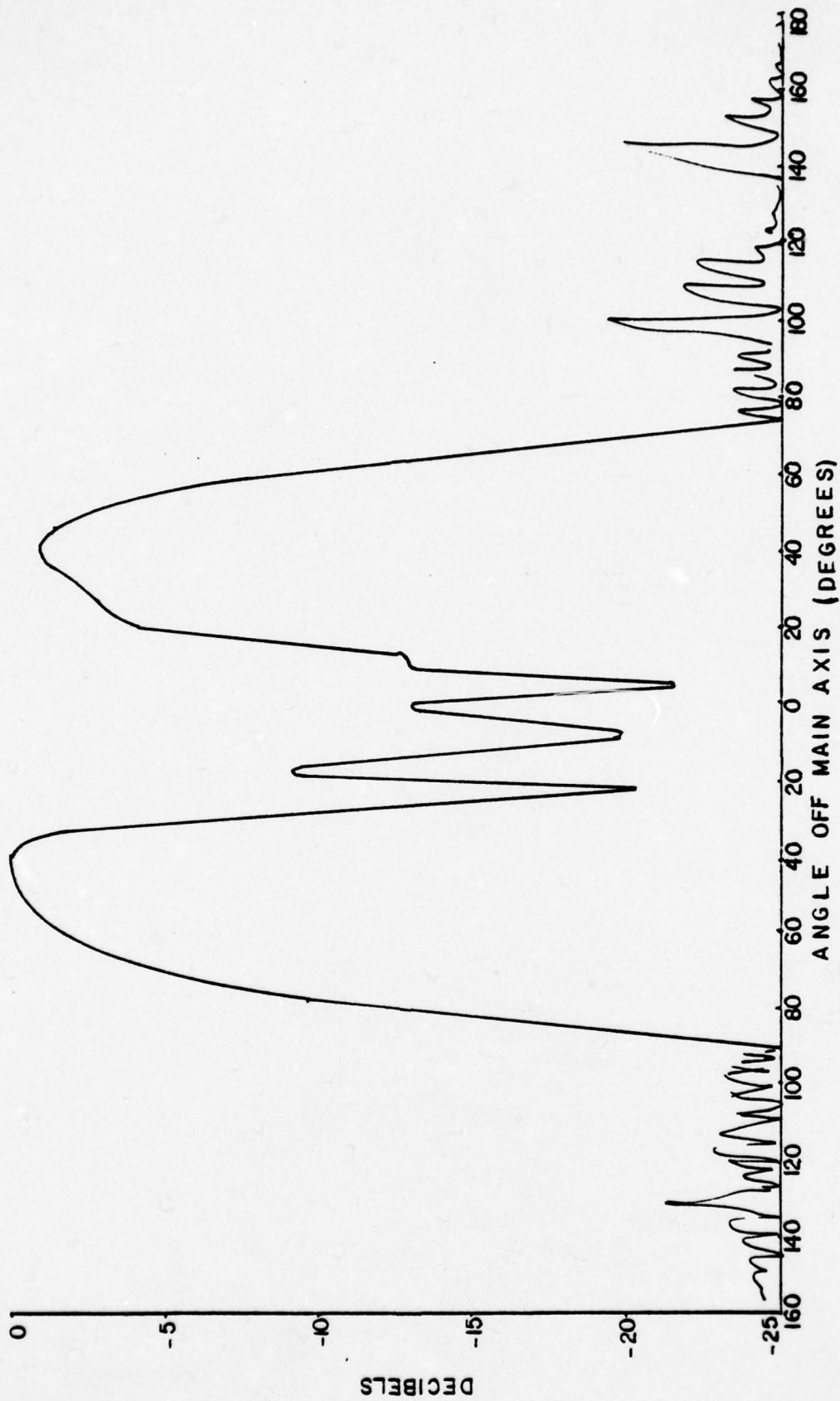
Figure 18 - BEAM PATTERN MOD 0 AT 72.4

DECIBELS
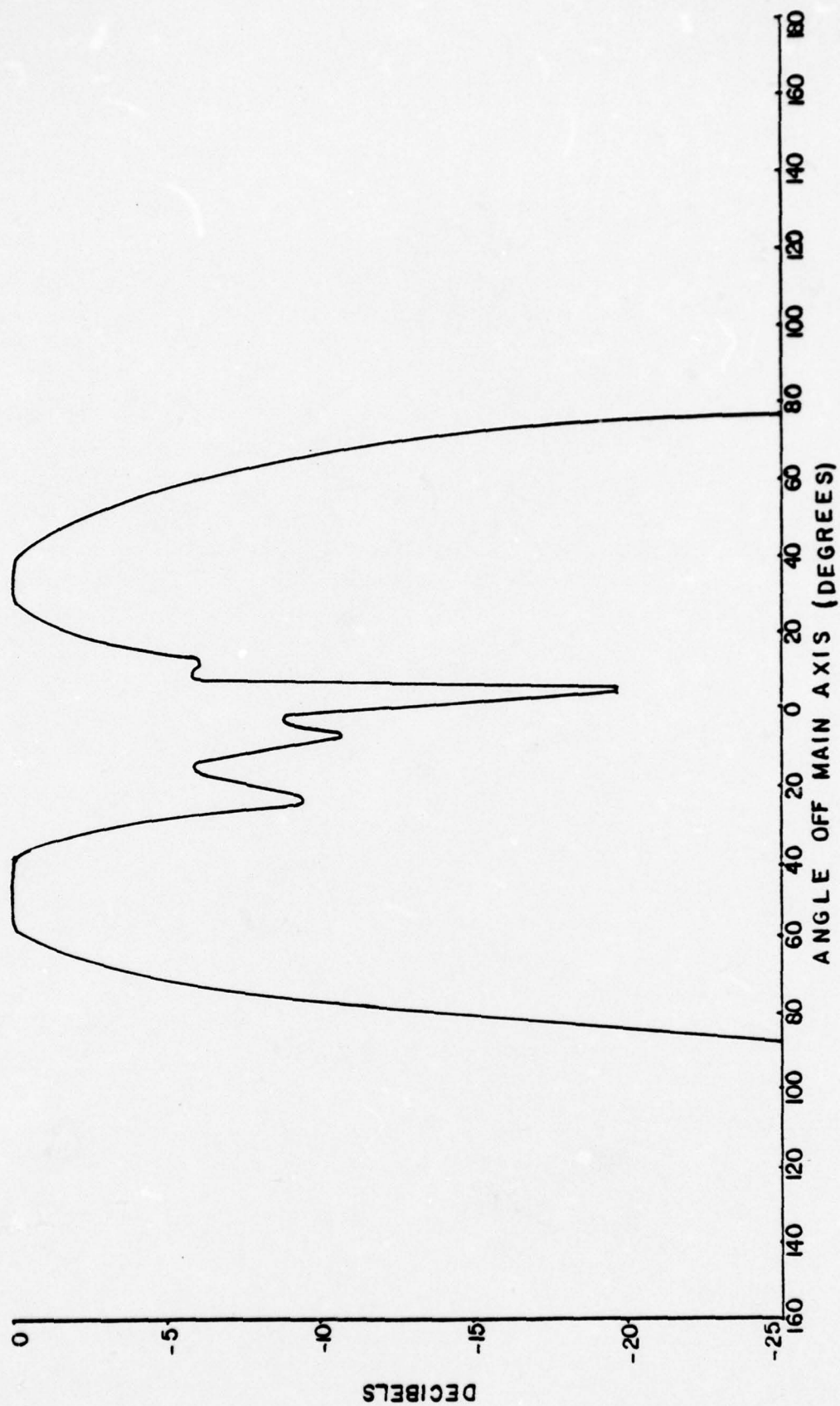
Figure 19 - BEAM PATTERN MOD 0 AT 79 kHZ

ANGLE OFF MAIN AXIS (DEGREES)

DECIBELS
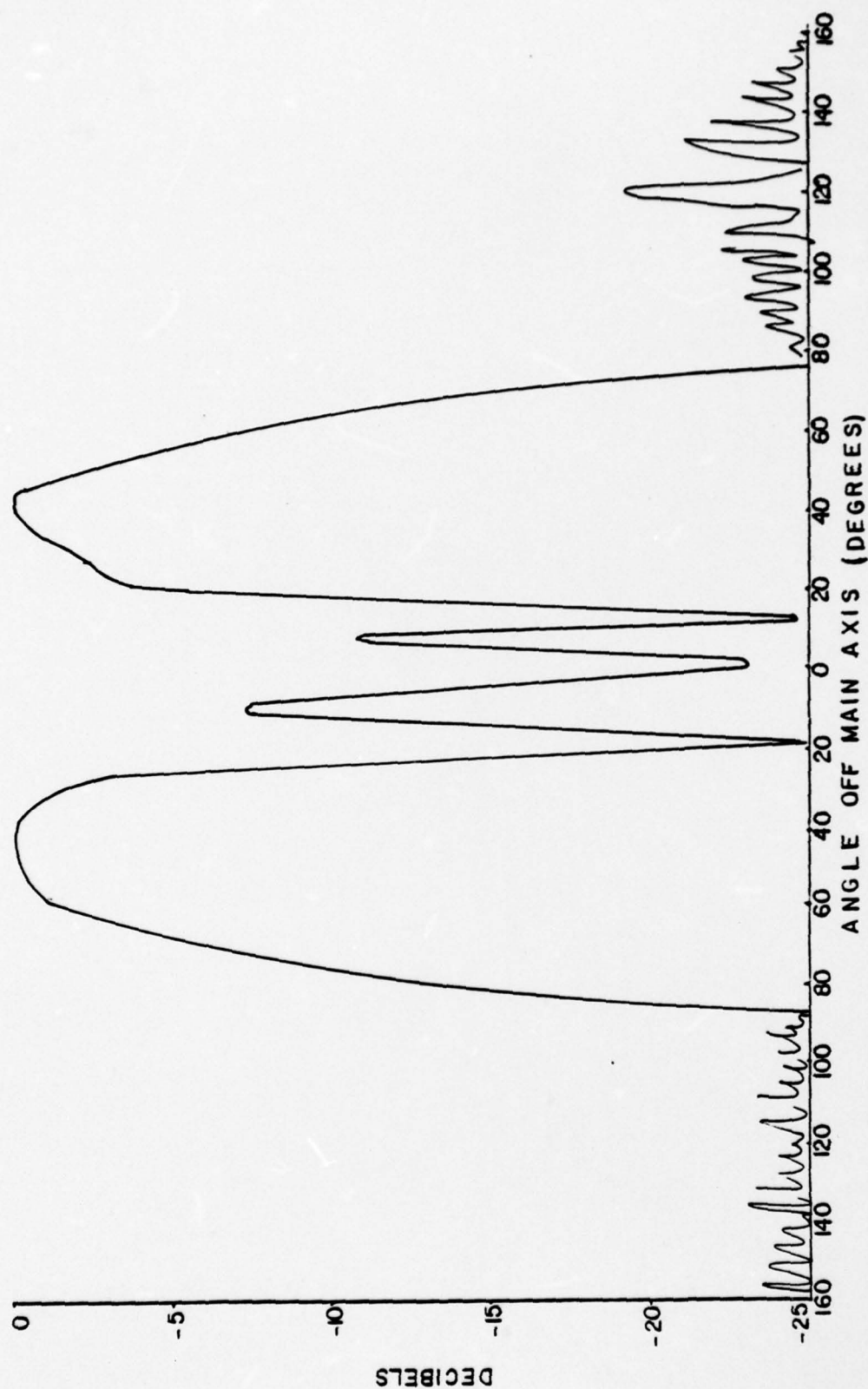
Figure 20 - BEAM PATTERN—RADIATORS DRIVEN INDEPENDENTLY

ANGLE OFF MAIN AXIS (DEGREES)

DECIBELS

INPUT · 25 VOLTS rr.

ANGLE OFF MAIN AXIS (DEGREES)

DECIBELS
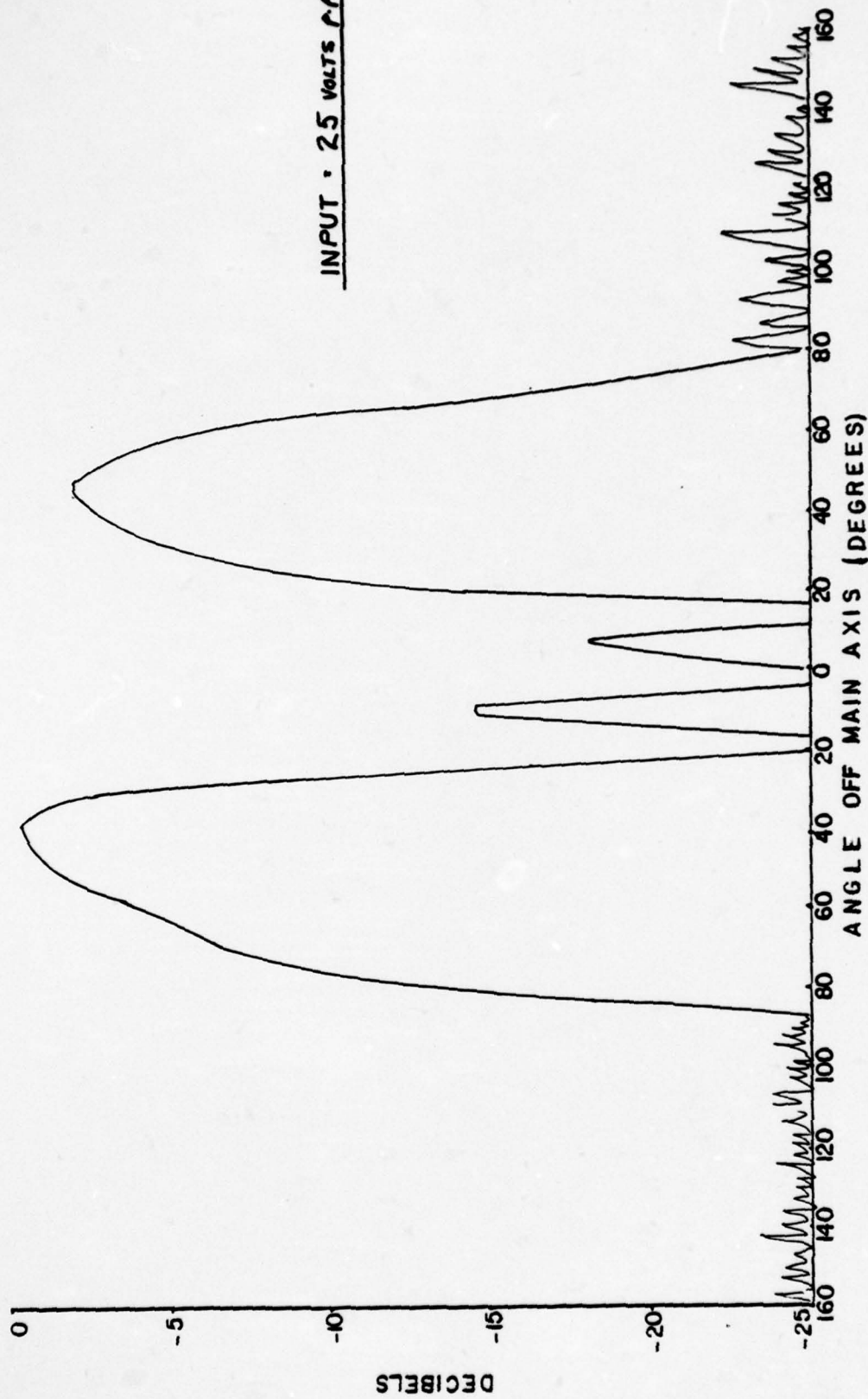
Figure 21 - BEAM PATTERN-INCREASING VOLTAGE DRIVE

40

INPUT = 60 VOLTS p-p

ANGLE OFF MAIN AXIS (DEGREES)

DECIBELS
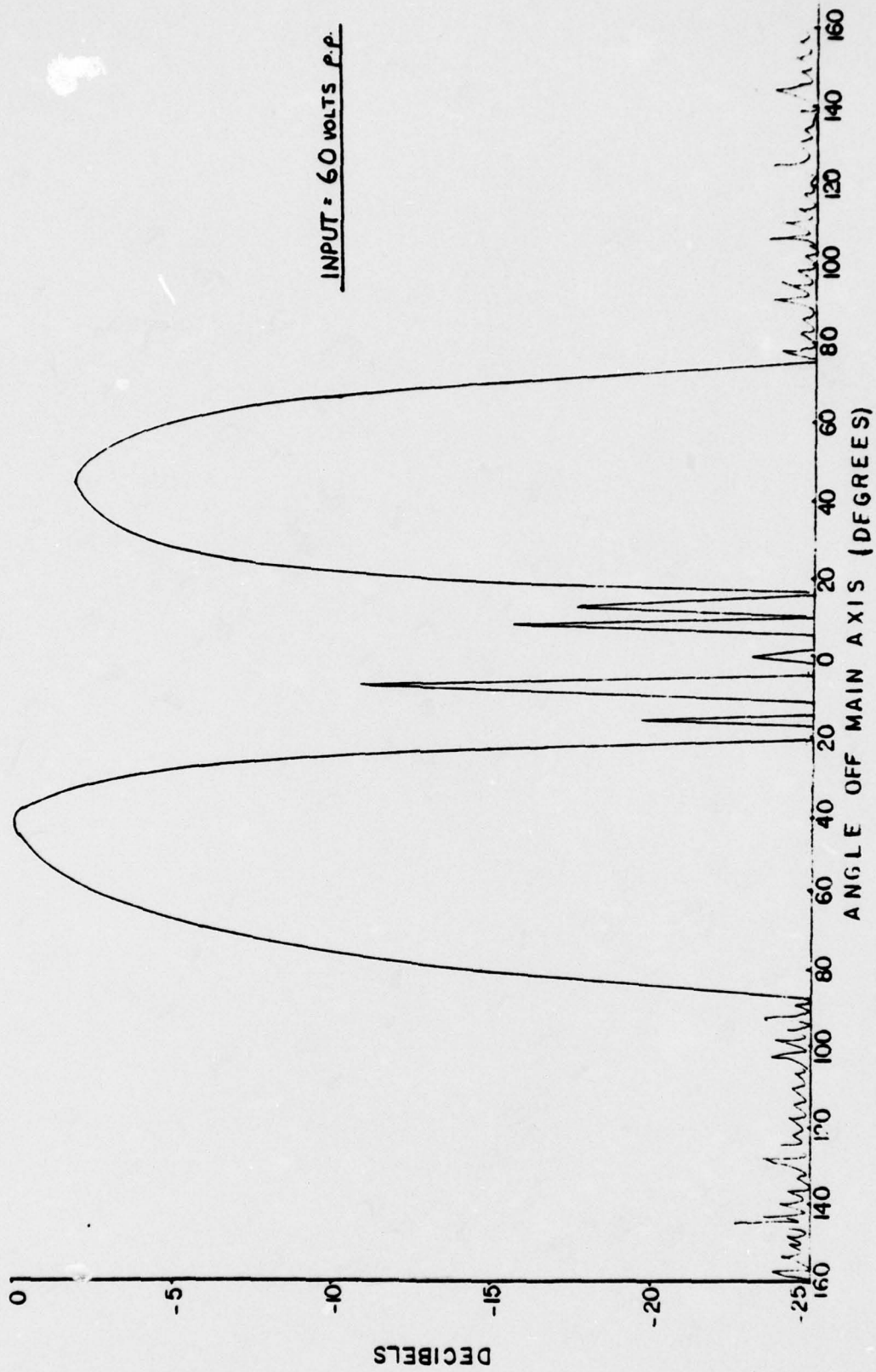
Figure 22 - BEAM PATTERN-INCREASING VOLTAGE DRIVE

41

INPUT = 95 VOLTS P.P.

ANGLE OFF MAIN AXIS (DEGREES)

DECIBELS
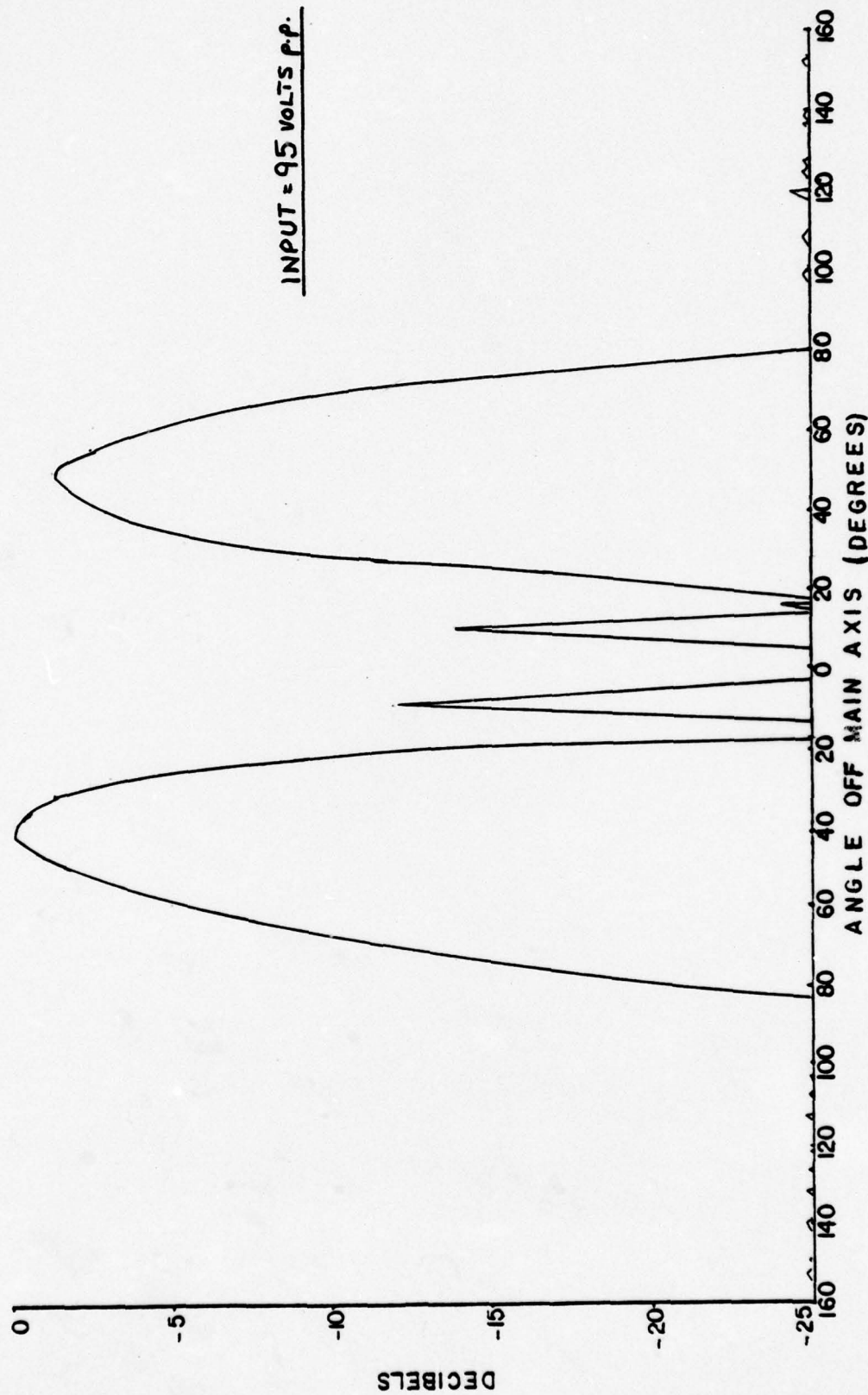
Figure 23 - BEAM PATTERN-INCREASING VOLTAGE DRIVE

42

INPUT = 130 volts P-P

ANGLE OFF MAIN AXIS (DEGREES)

DECIBELS
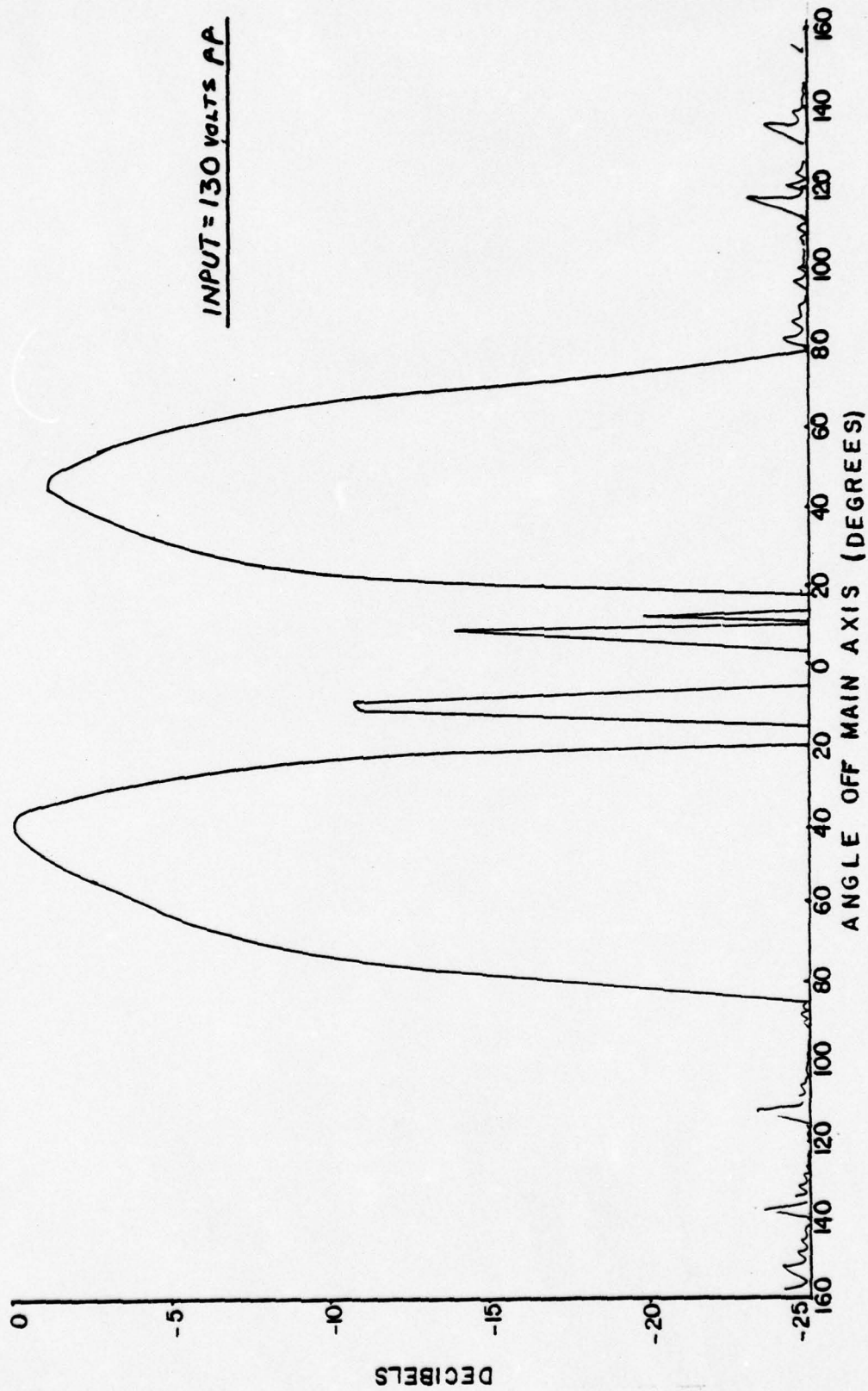
Figure 24 - BEAM PATTERN-INCREASING VOLTAGE DRIVE

43

INPUT = 165 VOLTS P.P.

ANGLE OFF MAIN AXIS (DEGREES)

DECIBELS
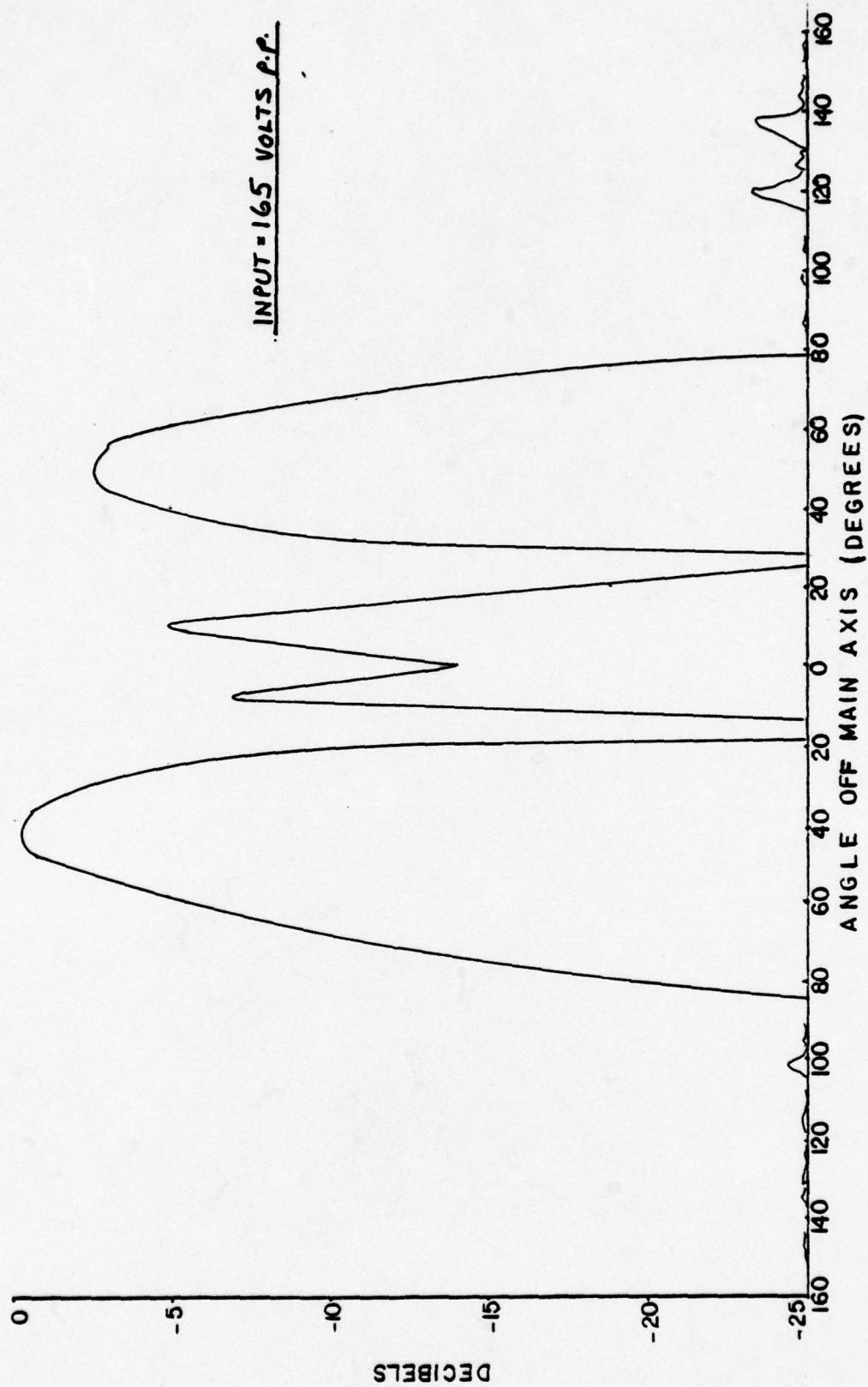
Figure 25 – BEAM PATTERN-INCREASING VOLTAGE DRIVE

44

INPUT = 200 VOLT P.P.

ANGLE OFF MAIN AXIS (DEGREES)

DECIBELS
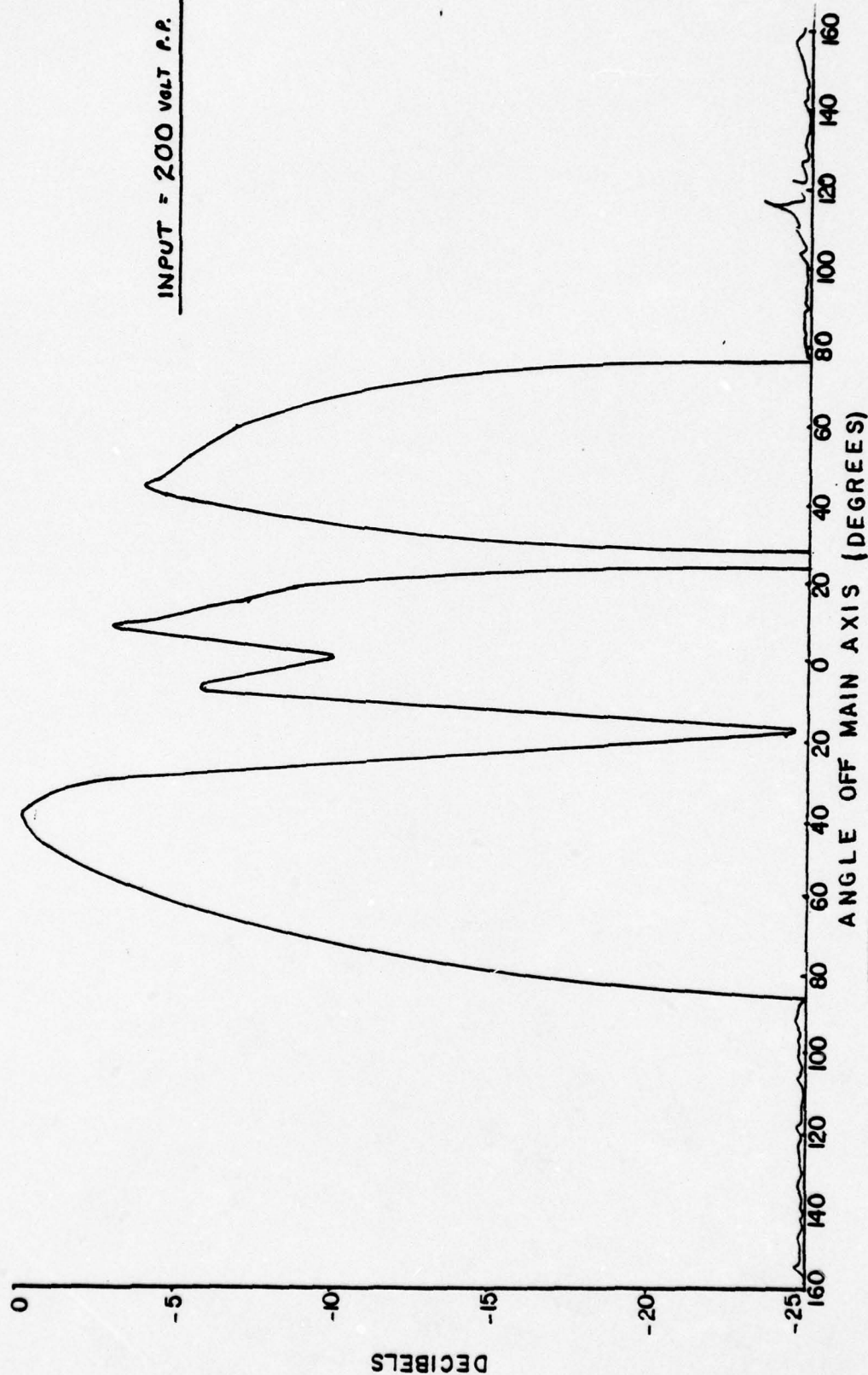
Figure 26 - BEAM PATTERN—INCREASING VOLTAGE DRIVE

45

INPUT = 270 VOLTS r.l.

ANGLE OFF MAIN AXIS (DEGREES)
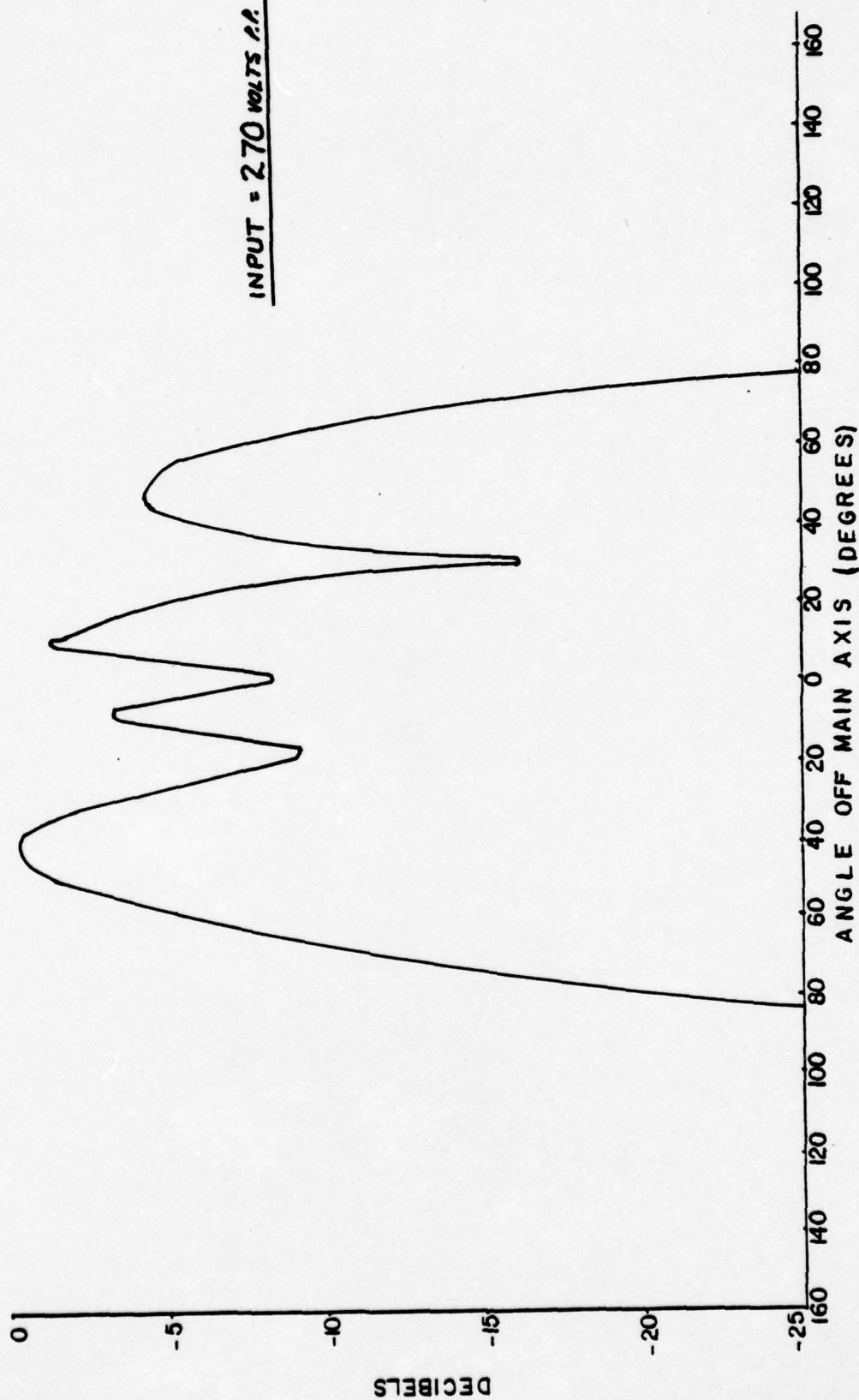
Figure 27 - BEAM PATTERN-INCREASING VOLTAGE DRIVE

DECIBELS

46

INPUT : 340 VOLTS P.P.

ANGLE OFF MAIN AXIS (DEGREES)
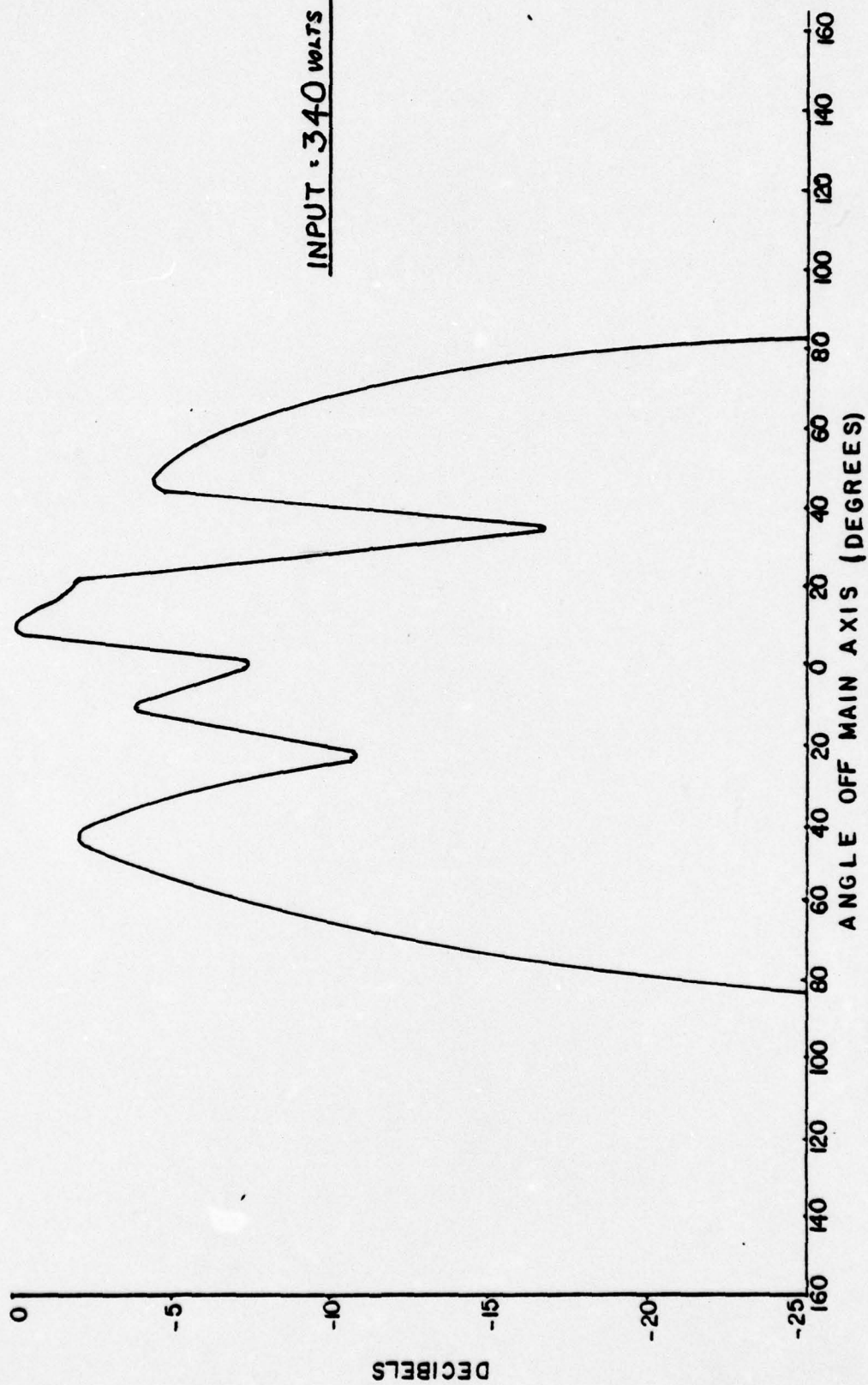
Figure 28 - BEAM PATTERN-INCREASING VOLTAGE DRIVE

DECIBELS

47

C. RADIATION TESTS OF TRANSDUCER ASSEMBLY MOD 1

Based on a more extensive study of computer calculated radiation patterns which permitted comparison of the effects of various combinations of radiating face dimensions and relative amplitude , it appeared likely that an improvement would result if the outer radius of the outer radiator was reduced by one quarter centimeter and its inner radius increased by one half centimeter. Due to the physical construction of Top Piece Mod 0, only one eighth centimeter could be taken off the outer diameter.

The dimensions of the newly machined Top Piece Mod 1 are shown in Fig. 29.

The first tests were of the linearity of response to increasing drive voltages. Beam patterns were recorded at the resonance frequency with equal drive voltages applied to both elements. Drive voltages were changed from 25 volts(p-p) to 340 volts(p-p). Typical patterns are presented in Fig. 30,31 and 32. The sound pressure levels increase linearly with drive voltage and,to within the accuracy of measurement (a few tenths of a db) over a range in excess of 20 iB. The relative amplitudes of the various portions of the beam and beamwidths appear to remain essentially independent of drive level.

The effect of frequency change on the beam pattern is presented in Fig. 33,34 and 35 in which the drive level was at the maximum available(340 volts p-p) with both elements driven in parallel. The effect of a 6 kHz change in frequency on either side of the resonance frequency appears to cause only minor changes in beamwidth and relative

48

amplitude of the central lobe and side lobes. At the highest frequency at which data were taken (84 kHz) there was some reduction in overall beamwidth with a concomitant increase in amplitude of the central lobe.

It is concluded that the Mod 1 transducer assembly is linear in its response with an acceptable beamwidth in the 12 Khz band centered at its resonance frequency.
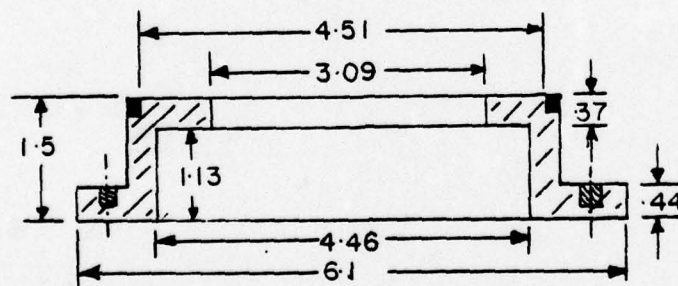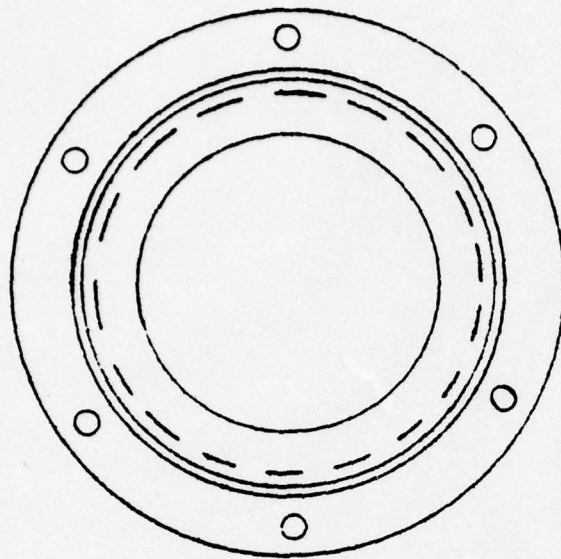
UNITS IN CENTIMETERS

Figure 29 - DIMENSIONS OF TOP PIECE MOD 1

73.6 KHz

INPUT: 25 VOLTS PP.

0 dB = 57.4 dB ref. 1 μbar.
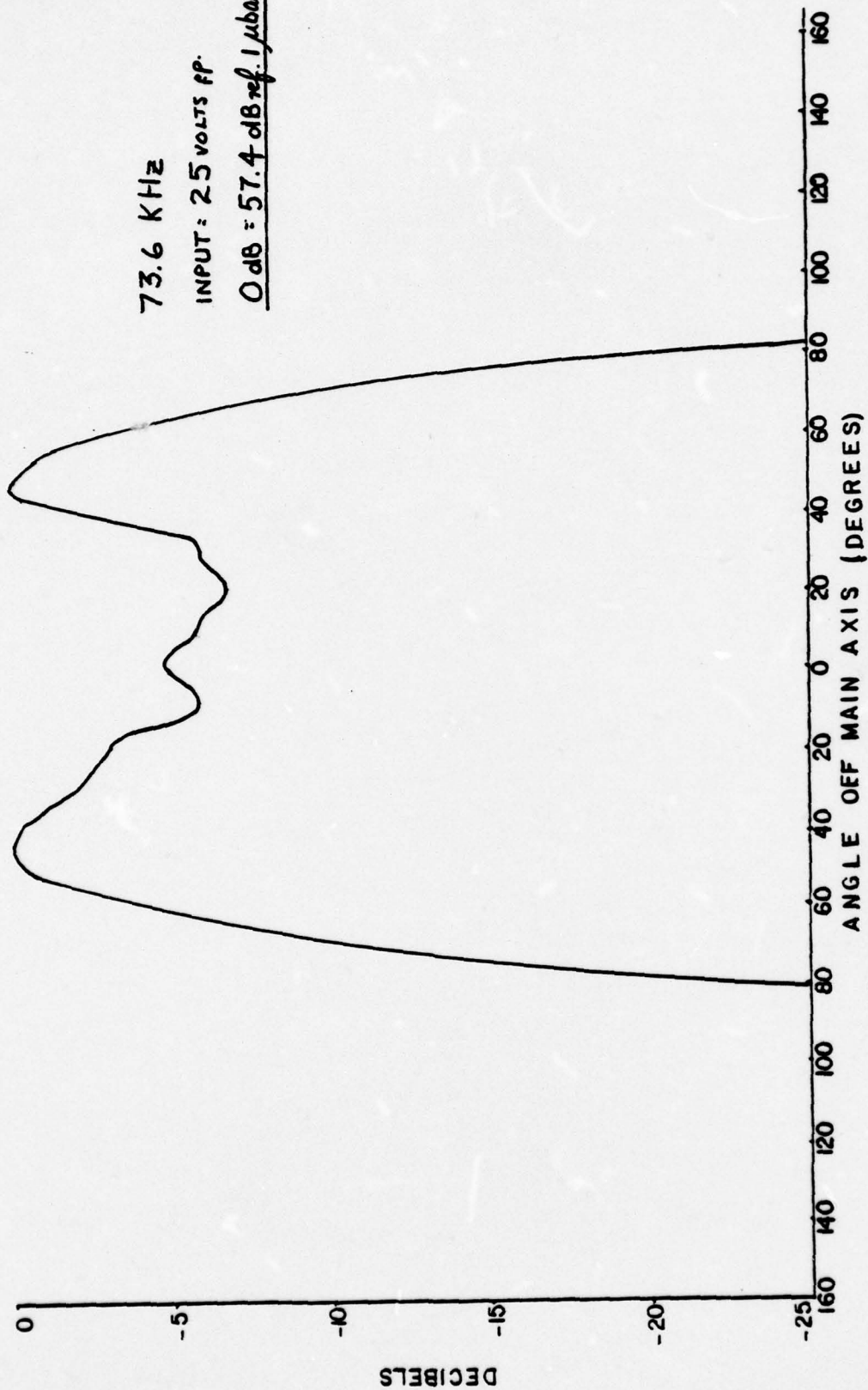
Figure 30 - BEAM PATTERN-ASSEMBLY MOD 1

ANGLE OFF MAIN AXIS (DEGREES)

DECIBELS

73.6 KHz
INPUT = 200 volts P.P.
0 dB = 76.1 dB ref 1 μbar

ANGLE OFF MAIN AXIS (DEGREES)

DECIBELS
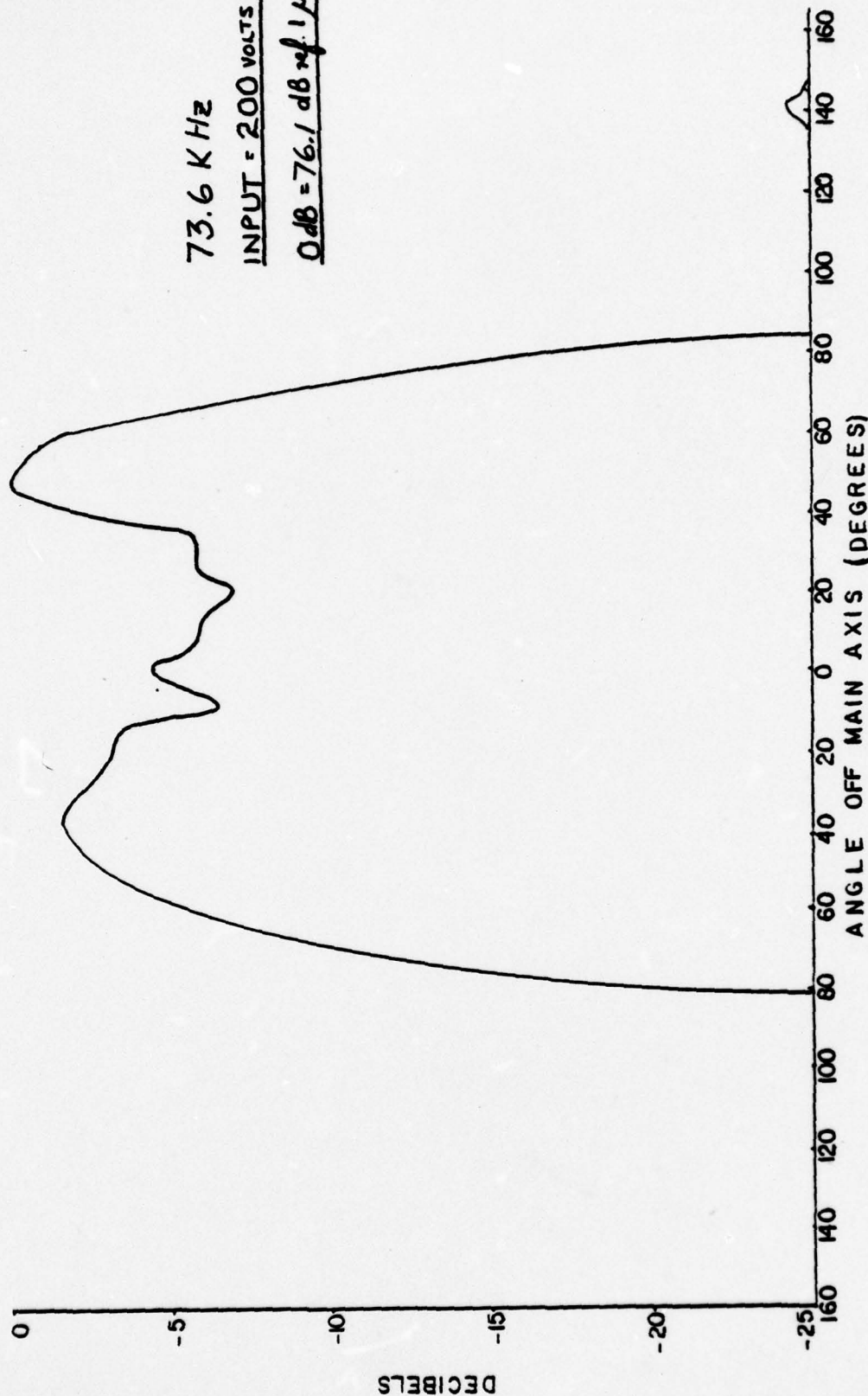
Figure 31 - BEAM PATTERN-ASSEMBLY MOD 1

52

73.6 KHz

INPUT = 340 VOLTS PP

0 dB = 79 dB ref 1 μbar

ANGLE OFF MAIN AXIS (DEGREES)

DECIBELS
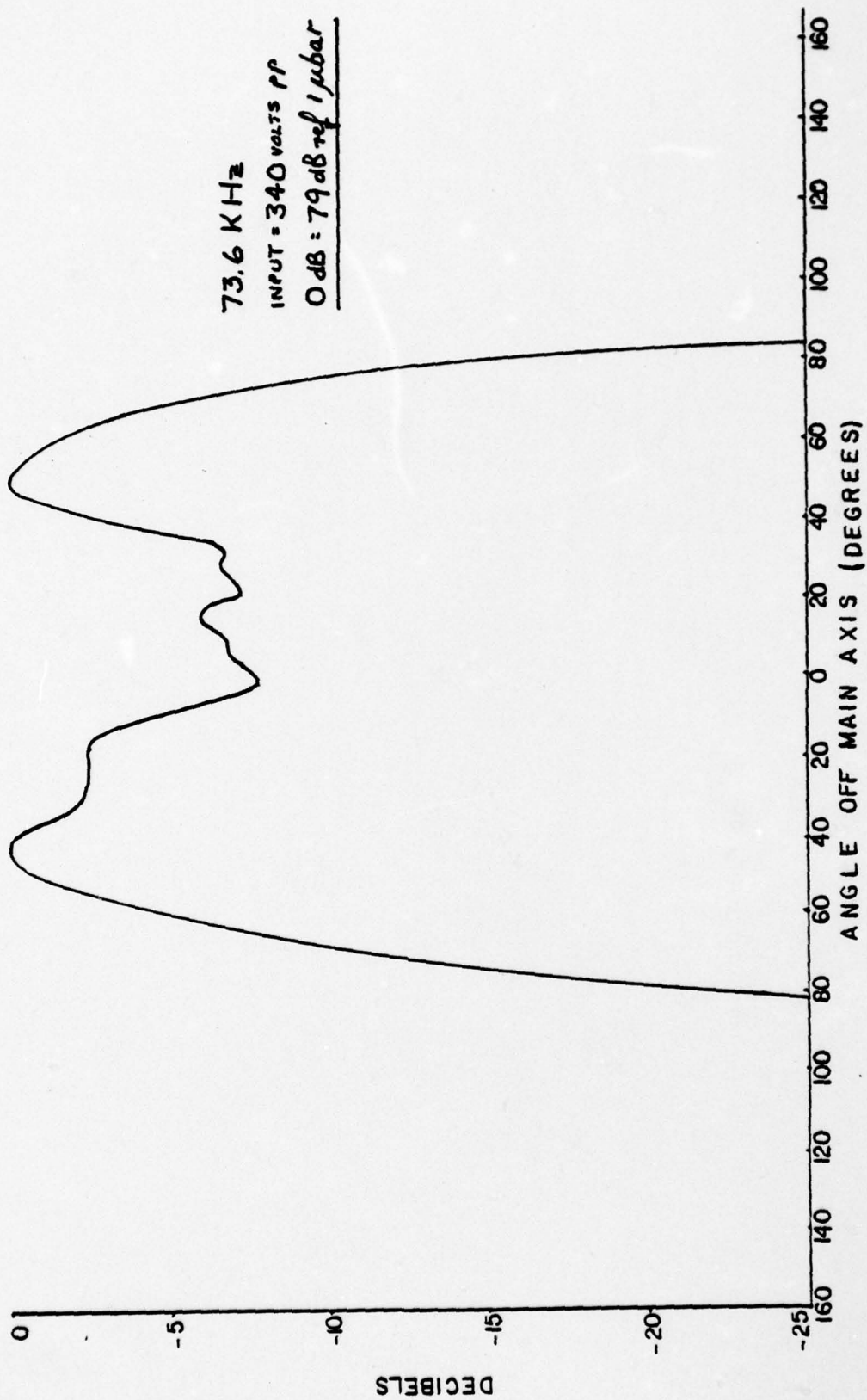
Figure 32 - BEAM PATTERN-ASSEMBLY, MOD 1

53

ANGLE OFF MAIN AXIS (DEGREES)
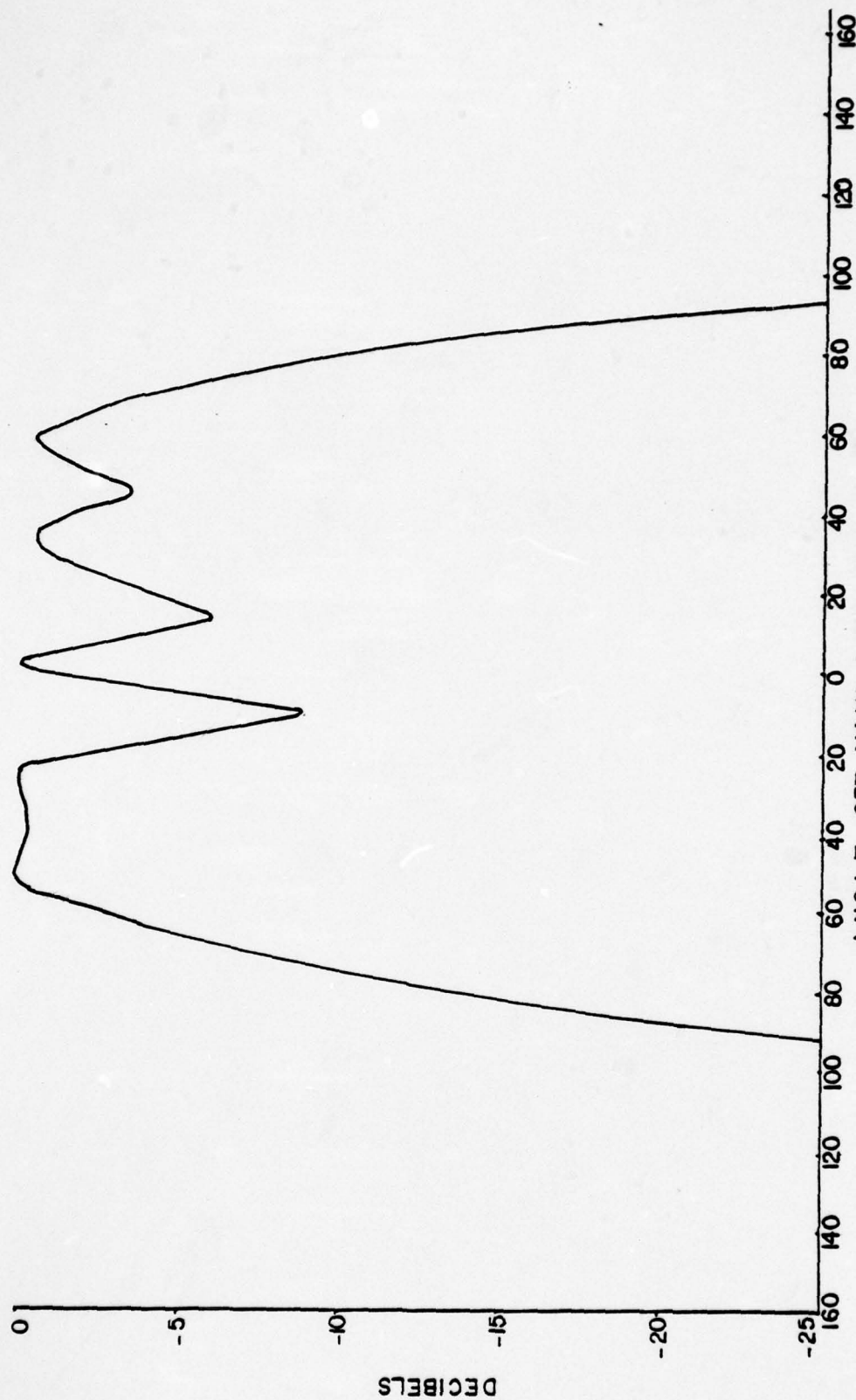
Figure 33 - BEAM PATTERN MOD 1 AT 66 KHZ

DECIBELS

ANGLE OFF MAIN AXIS (DEGREES)
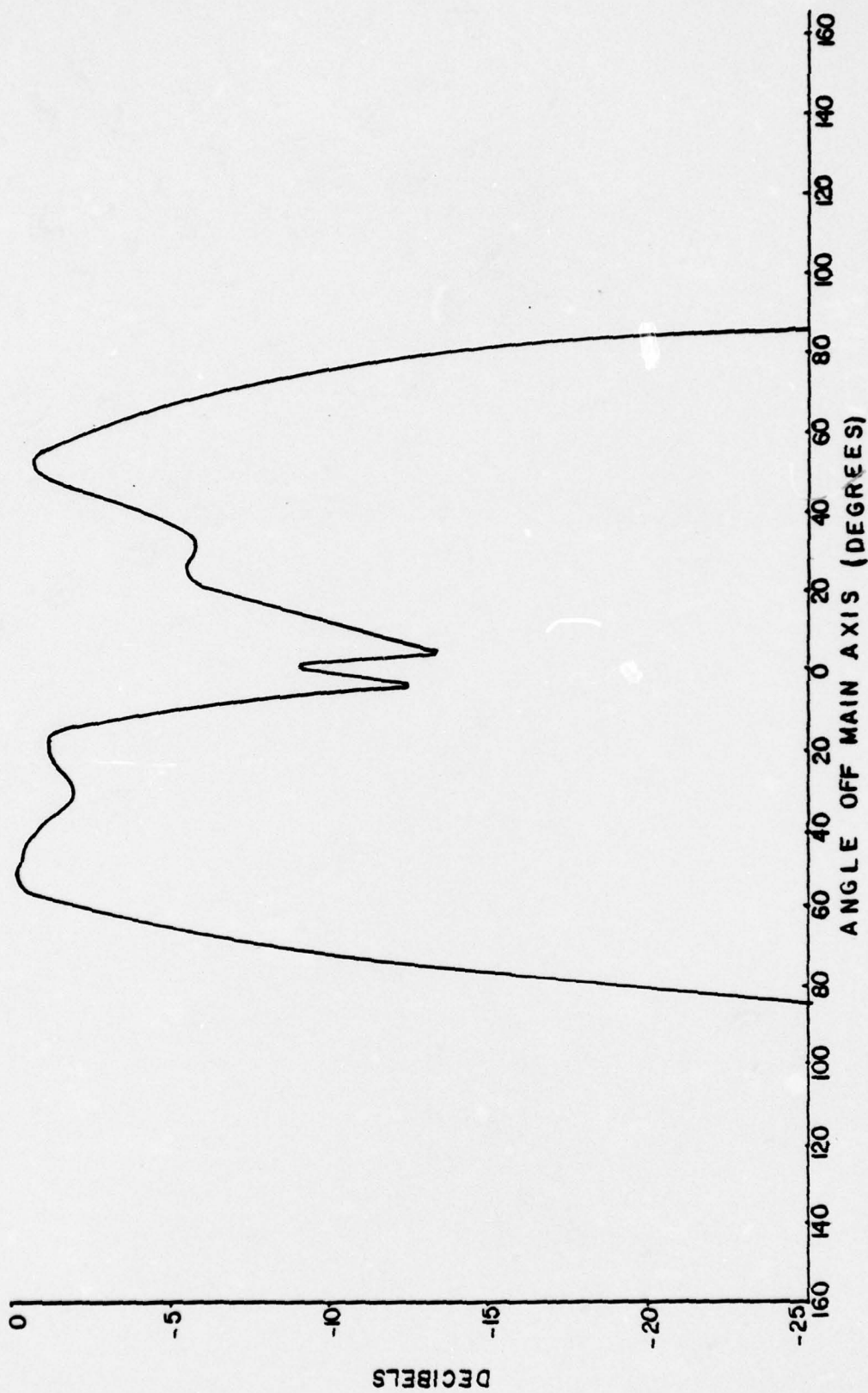
Figure 34 - BEAM PATTERN MOD 1 AT 72 KHZ

DECIBELS

55

ANGLE OFF MAIN AXIS (DEGREES)
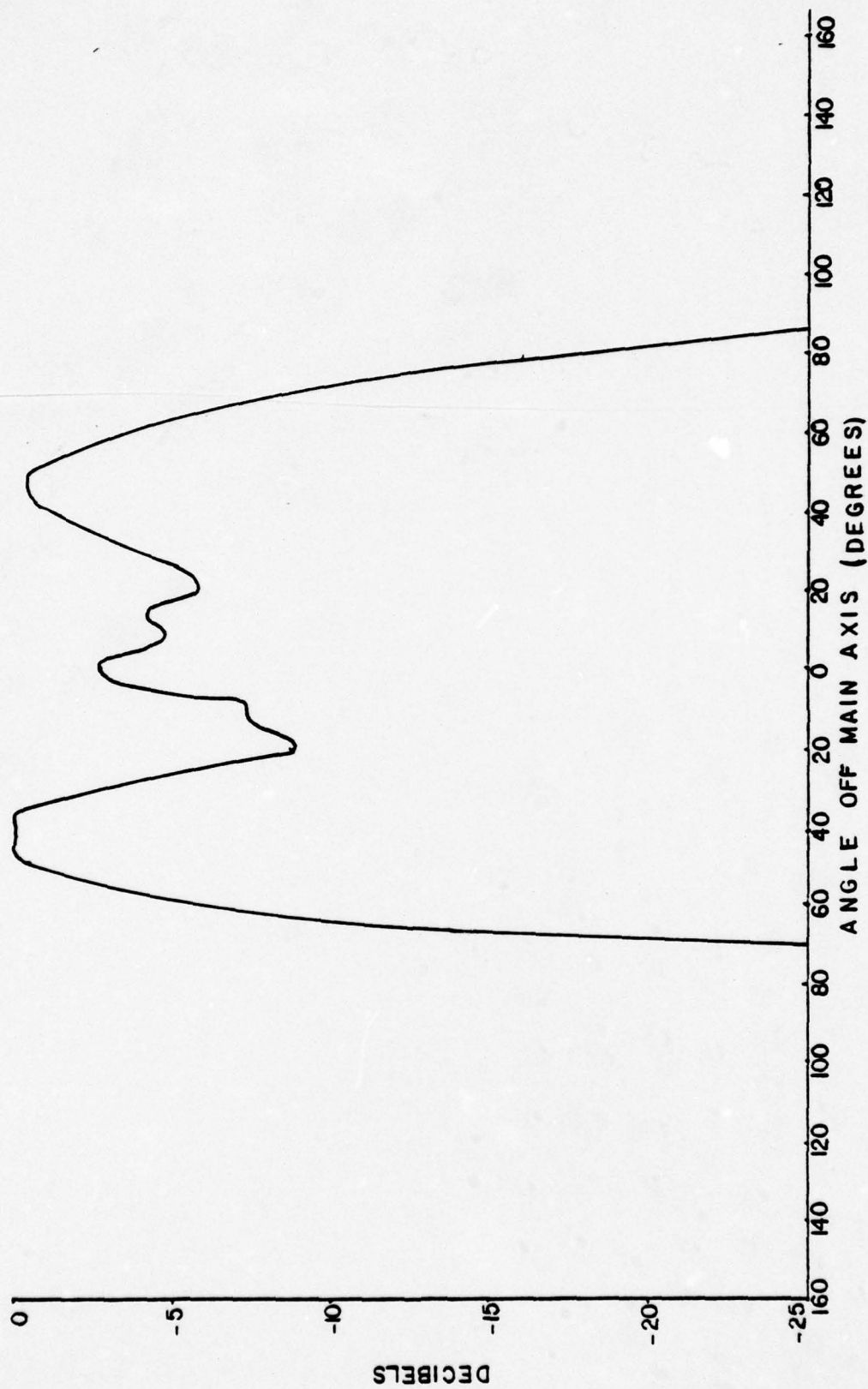
Figure 35 - BEAM PATTERN MOD 1 AT 78 KHZ

DECIBELS

D. RADIATION TESTS OF TRANSDUCER ASSEMBLY MOD 2

A second redesign of the vibrating system was made with two principal objectives:
1. A simpler and easier to machine structure.
2. A resonance frequency of 75 Khz.

The same ceramics and inner radiator were to be used. The result of this new design is the transducer assembly Mod 2, whose specifications are shown on Fig. 36.

The radiating face dimensions are the same as those of Mod 1 except that the outer radius was decreased by one eighth centimeter.

Admittance diagrams for the transducer assembly Mod 2 are attached as Figs. 37 to 39. It was interesting to note that the objective of increasing the frequency of resonance to 75 Khz was essentially reached.

Next the linearity of the transducer assembly was checked by progressively driving the radiators with a higher voltage. The results are slightly different from the Mod 1 results but still are considered to be satisfactory. A similar radiation pattern was recorded for each successively higher drive voltage, but the difference was that the level of sgnal strength of the minimums progressively increased with higher drive. These minimums at plus and minus 10 degrees off the main axis were at a mean value of 22 db below the major lobe strength for the lower drive voltage (8.5 volts rms). As the driving voltage was increased, these nulls similarly increased their strength nearly linearly, so that when the maximum of 115 volts rms

57

was applied they were only 10 db below the major lobes
signal level. Fig. 40 and 41 are attached to show the
radiation patterns for the extremities of the driving
voltages used. It can be noted here that the overall
beamwidth of Mod 2 is narrower than that of the Mod 1
assembly.

Next,while being driven at a voltage of 115 rms,a series
of recordings were taken at frequencies ranging from 64 to
84 Khz. An analysis of these indicates that the 12 db down
beamwidth again decreases with higher frequency,and as a
group, the radiation patterns are relatively flat and
indicate slight assymetry at the higher frequency end.

Tests of the effect of amplitude shading indicated that
a better pattern could be achieved with shading. Tests were
conducted using separate power amplifiers to drive each
radiator. The inner piston was driven constantly at a value
of 115 volts rms,and the drive to the outer radiator was
varied as necessary. It was found that the Transducer
Assembly Mod 2 operates most effectively for our purposes
when the inner element drive voltage is 1.5 times that of
the outer element. Figure 42 shows the pattern due to this
shading.

Some efforts were made toward achieving a better
electrical impedance match between the amplifiers and the
transducer elements by the use of series inductors to tune
out the blocked capacitance of the transducer elements. The
admittances at the resonant frequencies were measured and
the required inductances to tune out the blocked capacitive
susceptance for an optimal impedance were calculated. It
was demonstrated that this would indeed improve matching.
Variable inductors designed for laboratory use were
employed. Ideally this inductance should be provided by the
secondary winding of a matching transformer whose turns

ratio would be such as to match the remaining conductance to the output of the driving power amplifier. The lack of facilities and the time required to build appropriate transformers caused experimentation on this approach to be stopped.

TOP

BASE
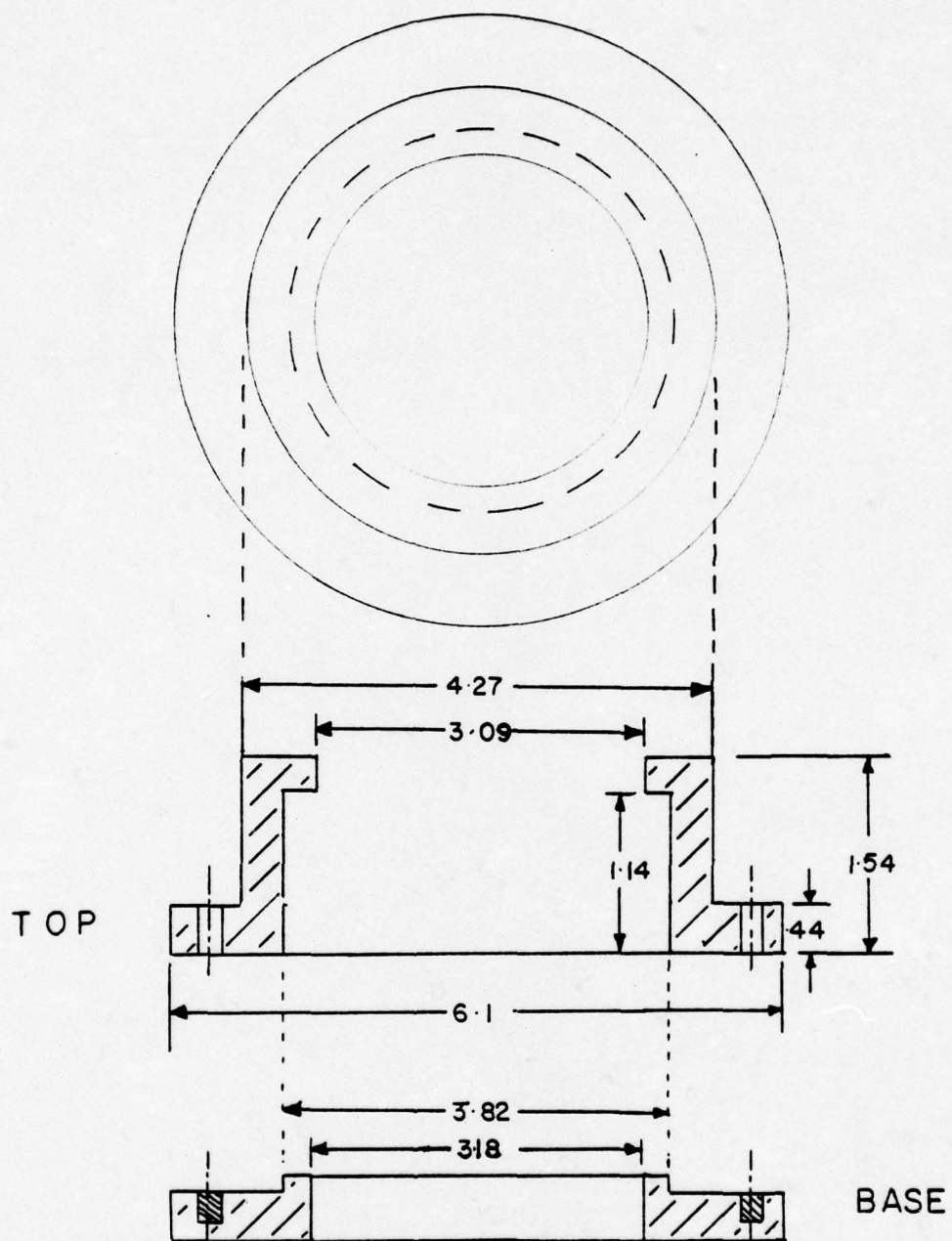
UNITS IN CENTIMETERS

Figure 36 - DIMENSIONS ASSEMBLY MOD 2

60

ADMITTANCE IN WATER

BOTH RADIATORS

MOD 2

$f_l = 70.9$ Khz

$f_r = 73.9$ Khz

$f_u = 76.8$ Khz

SUSCEPTANCE (MILLIMHOS)

CONDUCTANCE (MILLIMHOS)
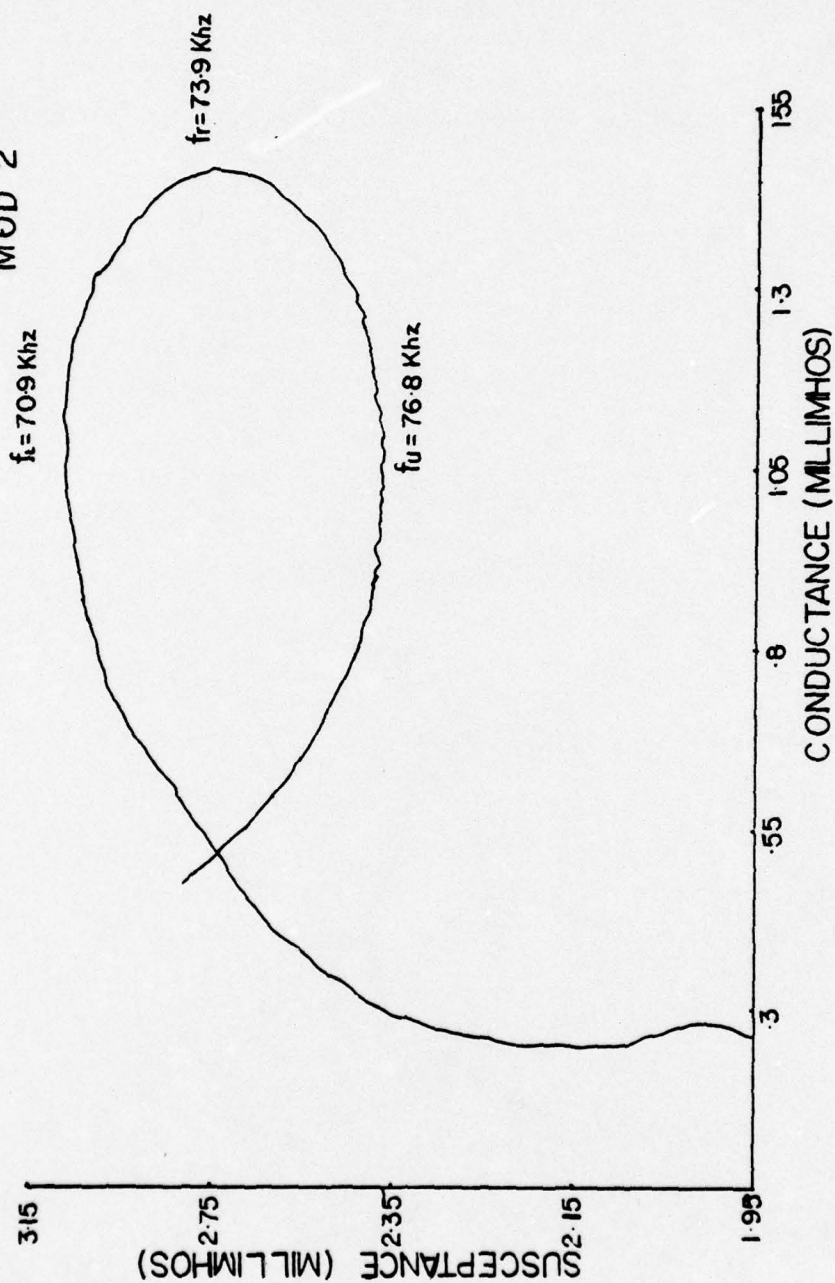
Figure 37 -: ADMITTANCE MEASUREMENTS-MOD 2

61

Figure 38 - ADMITTANCE MEASUREMENTS-MOD 2

ADMITTANCE IN WATER
INNER RADIATOR
MOD 2

$f_r = 74.9$ Khz

$f_L = 70.5$ Khz

$f_u = 79.2$ Khz

93K

SUSCEPTANCE (MILLIMHOS)

1·25

1·0

·75

·50

·25

·14   ·28   ·42   ·56   ·60

CONDUCTANCE (MILLIMHOS)
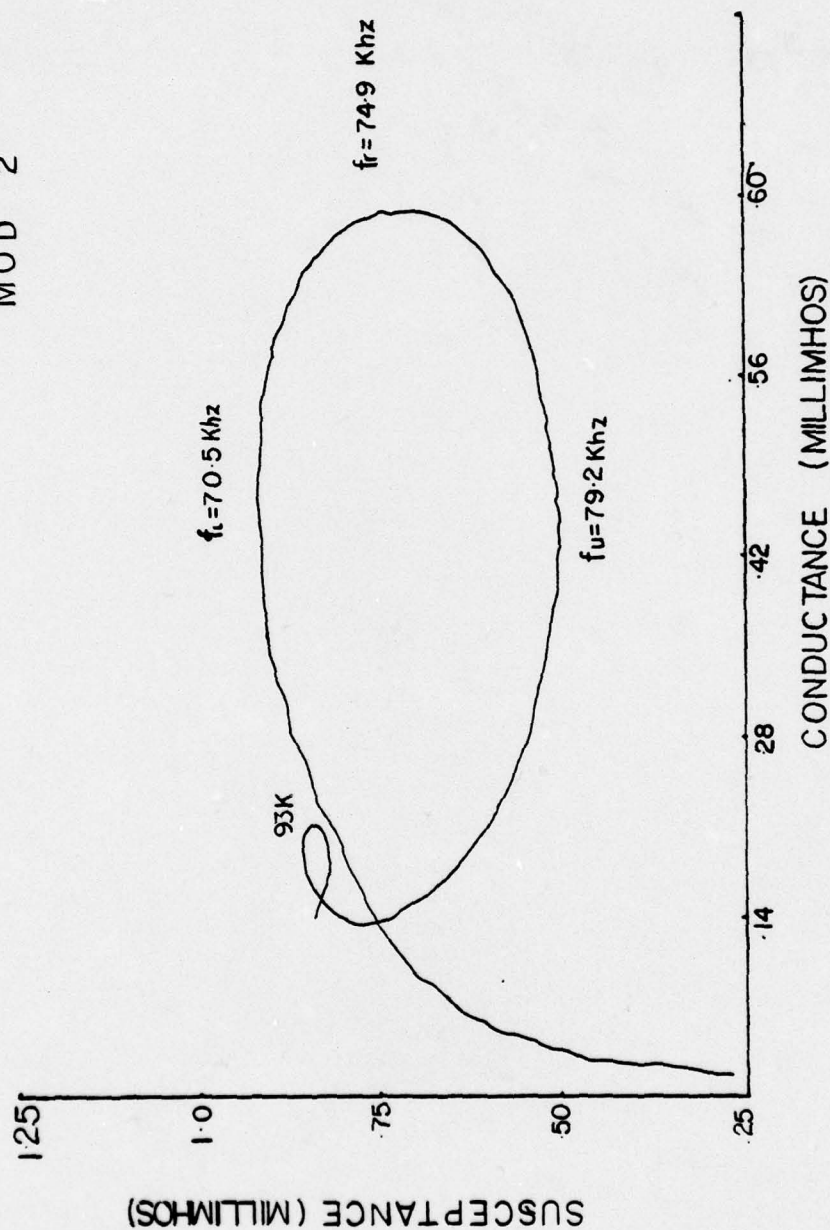
Figure 39 -. ADMITTANCE MEASUREMENTS-MOD 2

63

74 KHz - MOD 2

INPUT = 8.5 VOLTS RMS

ANGLE OFF MAIN AXIS (DEGREES)

DECIBELS
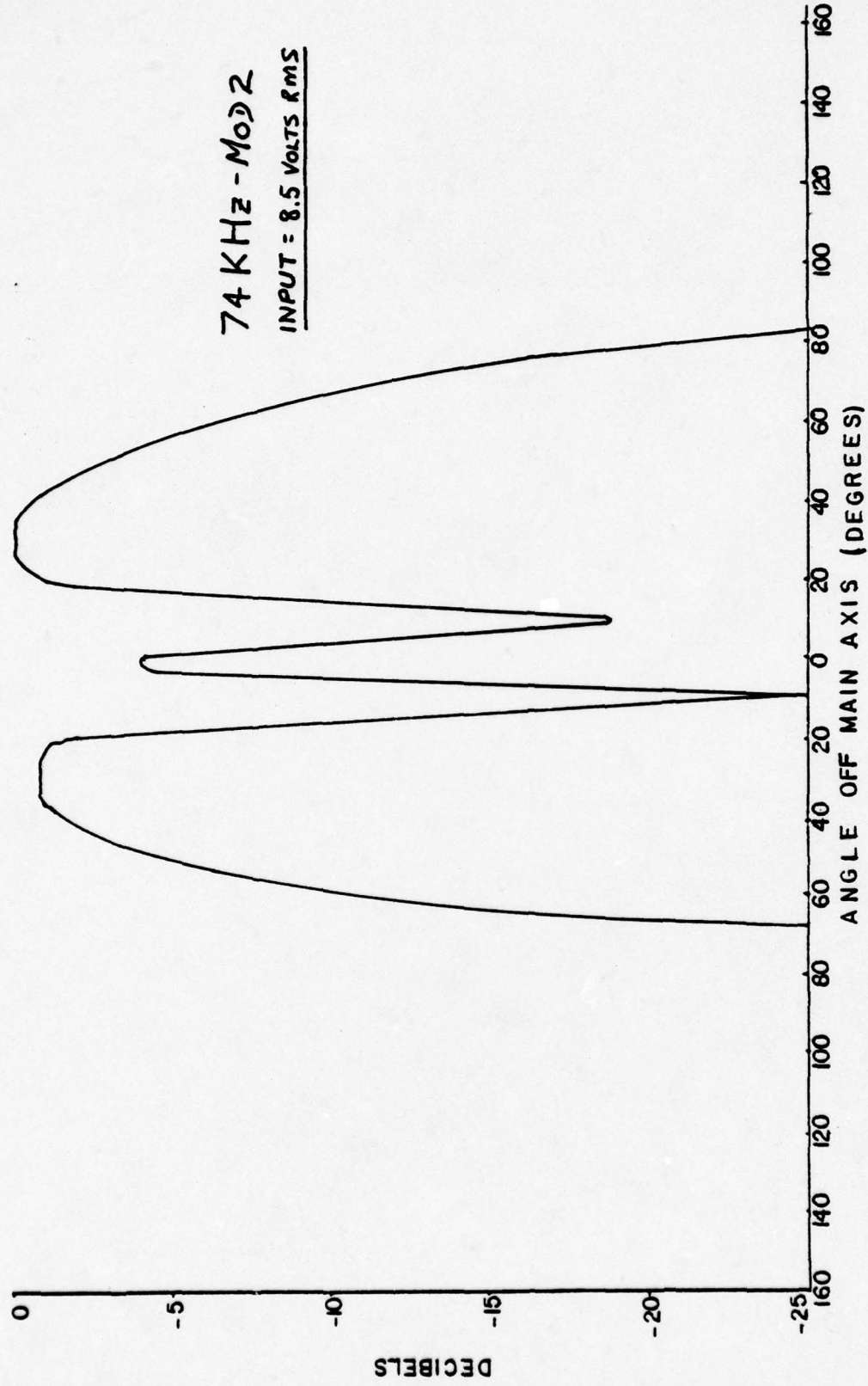
Figure 40 - BEAM PATTERN, MOD 2, LOW DRIVING VOLTAGE
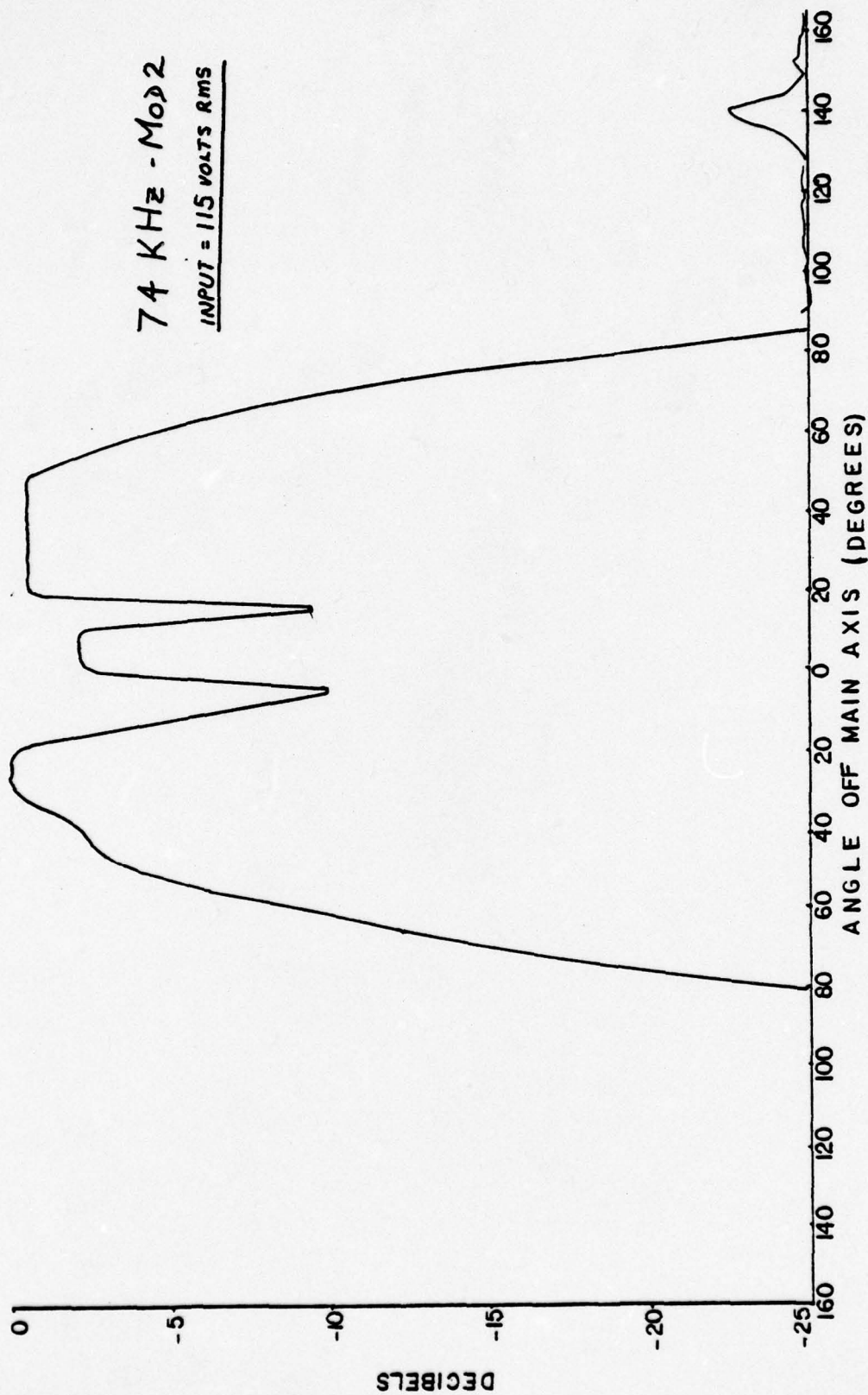
Figure 41 - BEAM PATTERN, MOD 2, HIGH DRIVING VOLTAGE

65
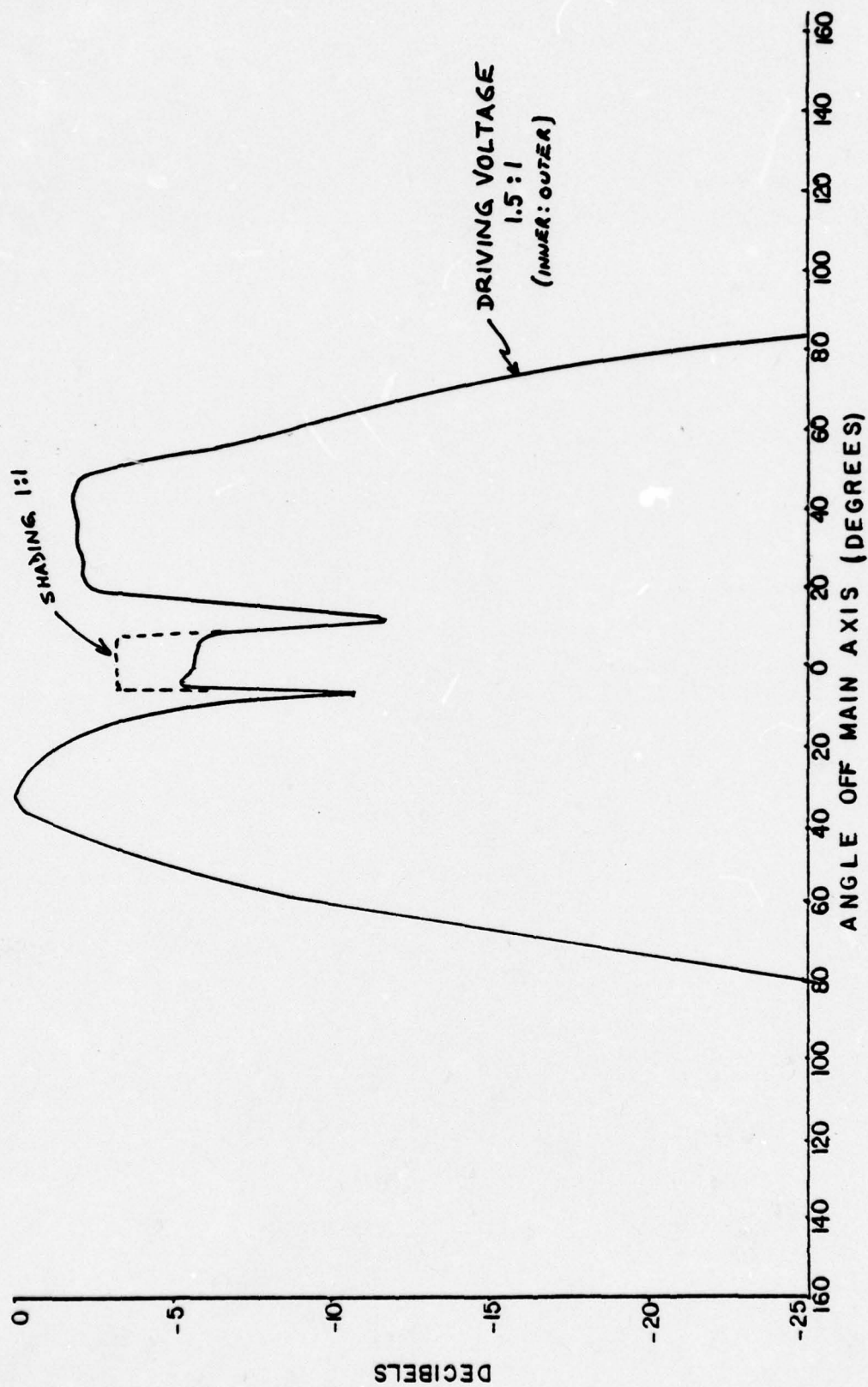
Figure 42 - BEAM PATTERN, COMPARISON DUE TO DRIVING VOLTAGE
SHADING

66

IV. SUMMARY,CONCLUSIONS AND RECOMMENDATIONS

A transducer assembly has been constructed with the objective to be compatible acoustically with the underwater range at the Naval Torpedo Station, Keyport and physically with the extender sections used with exercise torpedos.

The dimensions of the radiating faces were varied with the attempt to achieve a radiation pattern as in Fig. 3. The shape of the measured radiation patterns show much promise The maximum source level of 79 db reference one microbar at one meter was achieved with a peak power input of 20 watts. With proper impedance matching by the use of a transformer and with an appropriate and higher power output amplifier it is believed that the transducer assembly can achieve an acceptable source level and radiation pattern-with the strongest lobes at about 45 degrees off the main axis. Since this test transducer has a plane face,the curved face needed for hydrodynamic compatibility with high speed torpedos could be acieved by an appropriately shaped rubber cover.

It is recommended that further experimentation be done with this approach using the following steps:
1.Construct a new Top Piece whose radiating face dimensions are similar to those of Mod 1 assembly but with a shape like that of the Mod 2 Top Piece. This should make the radiation pattern as wide as the Mod 1 patterns but with the simplicity of Mod 2 construction.
2.Use Polyalkylene Glycol as the transducer liquid in accordance with Reference 2. This fluid is considered to be better than transformer or castor oil as a transducer

fluid-especially at high driving voltages.

3. Design and build an impedance matching transformer to match the intended power amplifier to the transducer assembly.

4. Conduct experiments on the effects of shading and phasing at high power drive.

5. Conduct final transducer tests at the Acoustic Test Facility at the Naval Torpedo Station at Keyport, Washington.

APPENDIX A

CONSIDERATIONS FOR BEAM PATTERN

Prior to the specification of the radiation pattern of a transducer, it is of interest first to analyze what portion of its operational environment should be insonified and then to determine the source level needed along each direction so that an optimum or practical pattern requirement can be specified.

The transducers used for acoustic ranging during weapons tests must insonify a number of arrays on the bottom of the test ranges. For a vehicle positioned a distance D from the bottom, the smallest propagation loss for transmission of sound occurs when the target vehicle and its transducer is directly above it. As the vehicle moves horizontally away from the array, the slant range increases with the angle between the vertical and the line to the array. The maximum slant range and maximum transmission loss to be considered occurs when the vehicle is equidistant between the first and the next array. The following expression gives the formula for transmission loss(TL):

$$TL = 20 \log r + ar \quad \text{decibels}$$

where r is the distance to the array and a is the absorption loss in db per yard.

If the distance to bottom D is considered, the slant range r can be related by the angle THETA between the vertical and the array by:

$$r = D/\cos(THETA)$$

The transmission loss is then calculated by

$$TL = 20 \ Log(D/\cos(THETA) + a(D/\cos(THETA))$$

A plot of the transmission loss verses the angle THETA is shown in Fig. 43 for a target vehicle distance from the bottom of D = 600 feet. The distance between arrays is considered to be 2500 yards.

In order that the arrays can expect a near constant sound pressure level when a vehicle is at a particular depth, it becomes apparent that the acoustic source level must increase with angle off the main axis of the transducer -which projects down from the transducer to the bottom of the test range. The dotted line on Fig. 43 indicates how the source level should increase with the angle THETA off the the transducer axis to compensate for the increasing transmission loss.

From the above analysis one can conclude that it is inefficient and not necessary to insonify the test range with a radiation pattern as in Fig. 1 and Fig. 2.

The acoustic power into the water could be reduced

70

significantly if the radiated energy could be focused into a solid angle of 40 to 75 degrees off the main axis. If the acoustic power could be reduced by 10 db in the solid cone bounded by 40 degrees off the transducer axis,the transducers acoustic power requirement would be reduced by approximately 25 percent. The resulting radiation pattern would be more efficient than the existing patterns and there would be the added benefit of a longer operational life due to the fact that lower driving voltages could be used. Various target vehicle distance to bottom D have been studied and the resulting recommended radiation pattern is attached as Fig. 44.

Figure 43 - ANGULAR DEPENDANCE OF TRANSMISSION LOSS

72

Figure 44 -: RECOMMENDED RADIATION PATTERN

73

APPENDIX B

RADIATION PATTERN COMPUTER PROGRAM

```
//ALNS6C7 JOB (O251,O46O,UX52),'AUNS 1780'
//FCRT.SYSIN CD*
C    DETERMINATION OF BEAM PATTERN FOR TWO CONCENTRIC TRANDUCERS
C    CONSISTING OF TWO COAXIAL RADIATORS.
C    THE INNER RADIATING FACE IS A PISTON OF RADIUS RI.
C    THE OUTER RADIATING FACE IS A CYLINDER OF INNER RACIUS ROI
C    AND OF CUTER RADIUS RO.
C
      DIMENSION XPDB(46),XAXIS(46)
    1 READ(5,100,END=3)RI,ROI,RO,UIN,UOUT,FREQ
  1CC FCRMAT(5F10.5,1F15.5)
      CC  N=1,5
      PHASE=180.0
      WRITE(6,200)RI,ROI,RO
      WRITE(6,201)UIN,UOUT,PHASE
      WRITE(6,202)FREQ
  2CC FCRMAT(//,2X,'RI=',2X,F10.5,2X,'RCI=',2X,F10.5,2X,'RC=',2X,F10.5)
  2C1 FCRMAT(//,'UIN=',F10.5,'UOUT=',F10.5,'PHASE=',F10.5)
  2C2 FCRMAT(//,2X,'FREG=',2X,F15.5)
      PI=3.14159
      FK=2.*PI*FREQ/1480.
      AKI=PK*RI
      AKCI=PK*ROI
      AKC=PK*RO
      PHASR=PHASE/57.29578
      PTZI=(UIN*(RI**2))*COS(PHASR)
      PTZCI=(UIN*(ROI**2)
      PTZCC=UOUT*(RO**2)
      PTZ=ABS(PTZO-PTZOI+PTZI)
      WRITE(6,300)PTZ
      WRITE(6,500)
  300 FCRMAT(//,2X,'AXIS PRESSURE',2X,E12.5)
  5CC FCRMAT(//,3X,'ANGLE','10X,'PRESSURE',14X,'CECIBEL')
      X=1.0
      N=2
      XFCE(1)=0.0
      XAXIS(1)=0.0
      CC 2 I=1,90,2
      AI=I
      TH=AI/57.29578
      ARGC=PK*RO*SIN(TH)
      CALL BESJ(ARGO,1,BJ,.1,IER)
      TERMO=PTZO*(2.*BJ/ARGO)
      ARGOI=PK*RCI*SIN(TH)
      CALL BESJ(ARGOI,1,BJ,.1IER)
      TERMOI=FTZOI*(2.*BJ/ARGOI)
      ARGI=PK*RI*SIN(TH)
```

```
      CALL BESJ(ARGI,1,BJ,1,IER)
      TERMI=PTZI*(2.*BJ/ARGI)
      PTI=TERMO-TERMOI+TERMI
      PCB=20.*ALOGIO(ABS(PTI/PTZI))
      XAXIS(M)=X
      XPCB(M)=PDB
      X=X+2.0
      M=M+1
  400 WRITE(6,400)I,PTI,PDB
      FORMAT(4X,I3,8X,E12.5,8X,F10.2)
    2 CONTINUE
      CALL PLOTP(XAXIS,XPCB,46,0)
      FREQ=FREQ-2000.0
    5 CONTINUE
    3 GO TO 1
      STOP
      END
C
C     SUBROUTINE BESJ
C
C     PURPOSE
C        COMPUTE THE J BESSEL FUNCTION FOR A GIVEN ARGUMENT AND ORDER
C
C     USAGE
C        CALL BESJ(X,N,BJ,D,IER)
C
C     DESCRIPTION OF PARAMETERS
C        X  - THE ARGUMENT OF THE J BESSEL FUNCTION DESIRED
C        N  - THE ORDER OF THE J BESSEL FUNCTION DESIRED
C        BJ - THE RESULTANT J BESSEL FUNCTION
C        D  - REQUIRED ACCURACY
C        IER- RESULTANT ERROR CODE WHERE
C             IER=0  NO ERROR
C             IER=1  N IS NEGATIVE
C             IER=2  X IS NEGATIVE OR ZERO
C             IER=3  REQUIRED ACCURACY NOT OBTAINED
C             IER=4  RANGE OF N COMPARED TO X NOT CORRECT (SEE REMARKS)
C
C     REMARKS
C        N MUST BE GREATER THAN OR EQUAL TO ZERO, BUT IT MUST BE
C        LESS THAN
C        20+10*X-X** 2/3    FOR X LESS THAN OR EQUAL TO 15
C        90+X/2             FOR X GREATER THAN 15
C
C     SUBROUTINES AND FUNCTION SUBPROGRAMS REQUIRED
C        NONE
C
C     METHOD
```

```
C     RECURRENCE RELATION TECHNIQUE DESCRIBED BY H. GOLDSTEIN AND
C     R.M. THALER,'RECURRENCE TECHNIQUES FOR THE CALCULATION OF
C     BESSEL FUNCTIONS',M.T.A.C.,V.13,PP.102-108 AND I.A. STEGUN
C     AND M. ABRAMOWITZ,'GENERATION OF BESSEL FUNCTIONS ON HIGH
C     SPEED COMPUTERS',M.T.A.C.,V.11,1957,PF.255-257
C     .................................................
C
      SUBROUTINE BESJ (X,N,BJ,D,IER)
C
      BJ = .0
      IF (N) 1,2,2
    1 IER = 1
      RETURN
    2 IF (X) 3,3,4
    3 IER = 2
      RETURN
    4 IF (X-15.) 5,5,6
    5 NTEST = 20.+10.*X-X**2/3
      GO TO 7
    6 NTEST = 90.+X/2.
    7 IF (N-NTEST) 9,8,8
    8 IER = 4
      RETURN
    9 IER = 0
      N1 = N+1
      BPREV = .0
C
C     COMPUTE STARTING VALUE OF M
C
      IF (X-5.) 10,11,11
   10 MA = X+6.
      GO TO 12
   11 MA = 1.4*X+60./X
   12 MB = N+IFIX(X)/4+2
      MZERO = MAXO(MA,MB)
C
C     SET UPPER LIMIT OF M
C
      MMAX = NTEST
C
      DO 21 M=MZERO,MMAX,3
C
C     SET F(M),F(M-1)
C
      FM1 = 1.0E-28
      FM = .0
      ALPHA = .0
```

33
34
35
36
37
38
39
40
41
42
43
44
45
46
47
48
49
50
51
52
53
54
55
56
57
58
59
60
61
62
63
64
65
66
67
68
69
70
71
72
73
74
75
76
77
78
79
80

```
   13  IF (M-(M/2)*2) 14,13,14
   14  JT =-1
       GC TO 15
   15  JT = 1
   15  M2 = M-2
C
       CC 18 K=1,M2
       MK = M-K
       BMK = 2.*FLOAT(MK)*FM1/X-FM
       FM1 = FM1
       FM1 = BMK
       IF (MK-N-1) 17,16,17
   16  EJ = BMK
   17  JT = -JT
   18  ALPHA = ALPHA+BMK*S
C
       BMK = 2.*FM1/X-FM
   19  BJ = BMK
       IF (N) 20,19,20
   20  ALPHA = ALPHA+BMK
       EJ = BJ/ALPHA
       IF (ABS(BJ-BPREV)-ABS(C*BJ)) 22,22,21
   21  BPREV = BJ
C
   22  IER = 3
       RETURN
       ENC
//GC.SYSIN DC *
```

81
82
83
84
85
86
87
88
89
90
91
92
93
94
95
96
97
98
99
100
101
102
103
104
105
106
107
108

APPENDIX C

MEASUREMENT PROCEDURES

A. VIBRATION MODE IDENTIFICATION

During the initial tests on Mod 0, a capacitive type displacement probe was used to help identify the vibrational modes and, in particular to determine the longitudinal mode. A thin resilient gasket on the face of the probe permits the motion of the radiating face to change the spacing between itself and the probe pick-up face. This results in a varying capacitance and causes a varying output. The system is schematically illustrated in Fig. 45.

By moving the probe around the cylindrical radiating face and observing the changes in probe output amplitude and phase (using a Lissajou pattern), the longitudinal mode was identified.
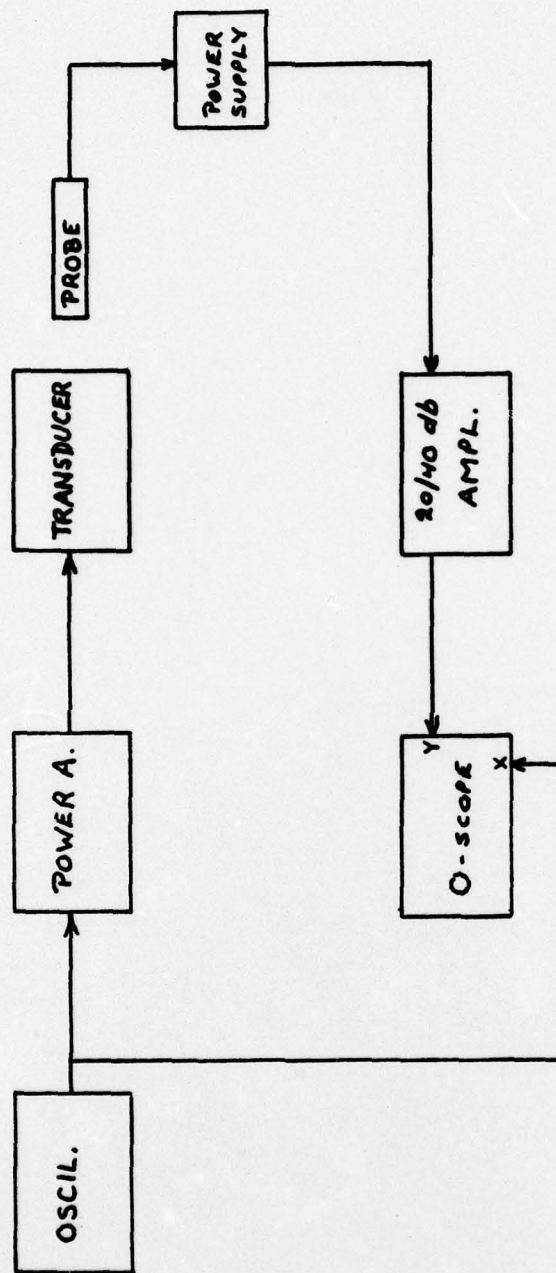
Figure 45 -: VIBRATION MODE IDENTIFICATION

79

B. ADMITTANCE DIAGRAMS

Throughout the design and construction phase electrical admittance measurements were taken using a DRANETZ (Model 100-C) ADMITTANCE METER in order to be able to determine the mechanical resonances of the vibrating system of concern. The mechanical resonances, may they be radial, thickness or longitudinal modes- are indicated on the admittance diagram as a point of maximum conductance. the combination of this technique to find various frequencies of mechanical resonance and the vibration mode identification mentioned in the previous section resulted in a methodical and accurate method to identify the desired resonant frequencies.

Admittance diagrams were generally made covering a frequency range of 20 to 100 Khz and the measurements were made both in water and air to determine the effect of the different radiation impedances offered by these mediums.

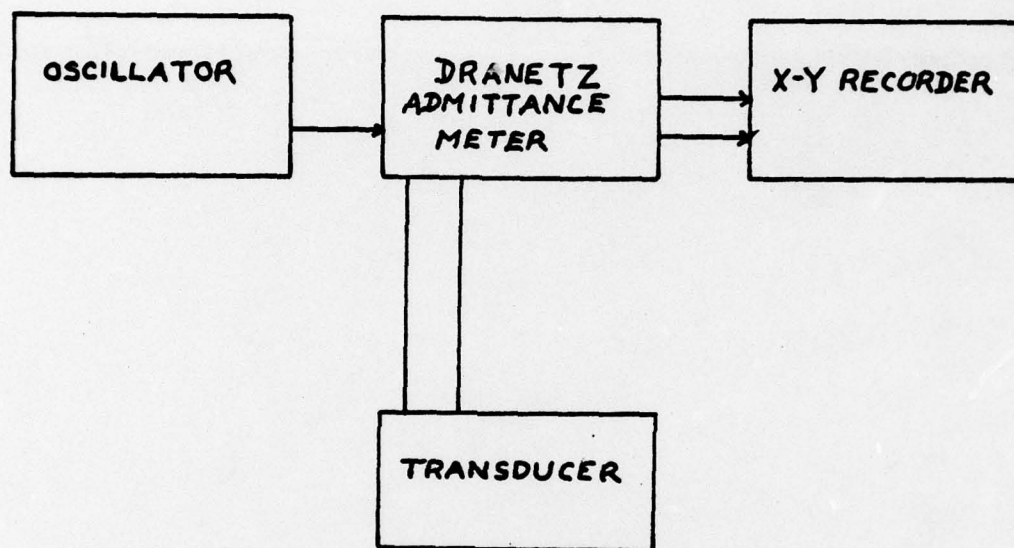Fig. 46 is attached to provide a schematic of the equipement used.

Figure 46 - EQUIPMENT FOR ADMITTANCE MEASUREMENT

OSCILLAT   RECORDER

Figure -3-   ASSEMBLY

C. BEAM PATTERN MEASUREMENTS

Fig. 47 is attached to give a schematic diagram of the equipment used during the beam pattern measurements. All the measurements were made in the anechoic tanks of Spanegal Hall Rm. 025. Pulsed transmissions were used in all cases so that the direct path pulse could be separated in time from the surface reflected pulse.

For the ease of plotting , the transducer assembly was rotated continually at six degrees per second during each recording run. A potentiometer on the gear train produced a d.c. voltage proportional to the angular position which was applied to the x-axis of an x-y recorder. The pick-up microphone was a calibrated LC10 hydrophone the output of which was amplified,rectified by an envelope detector and the connected to a P.A.R. MOD 160 Boxcar Integrator. This instrument was used in such a way that a time delayed gate which permits only the signal due to the direct acoustic path to be integrated. The integrator provides as an output a d.c. voltage which is proportional to the average amplitude of the demodulated pulse. The integrator provided a d.c. voltage as an output which was proportional to the average amplitude of the demodulated pulse.

A HP7561A Logarithmic Converter was used in order that the recorder could cover the large dynamic range of received signals on the same scale. This output was applied to the y-axis of the recorder.

The attenuator seen in fig. 47 was used to calibrate the x-y recording. This was especially necessary at signal levels of -20 db or less relative to the main lobe strength since it was found that this decibel scale was not linear
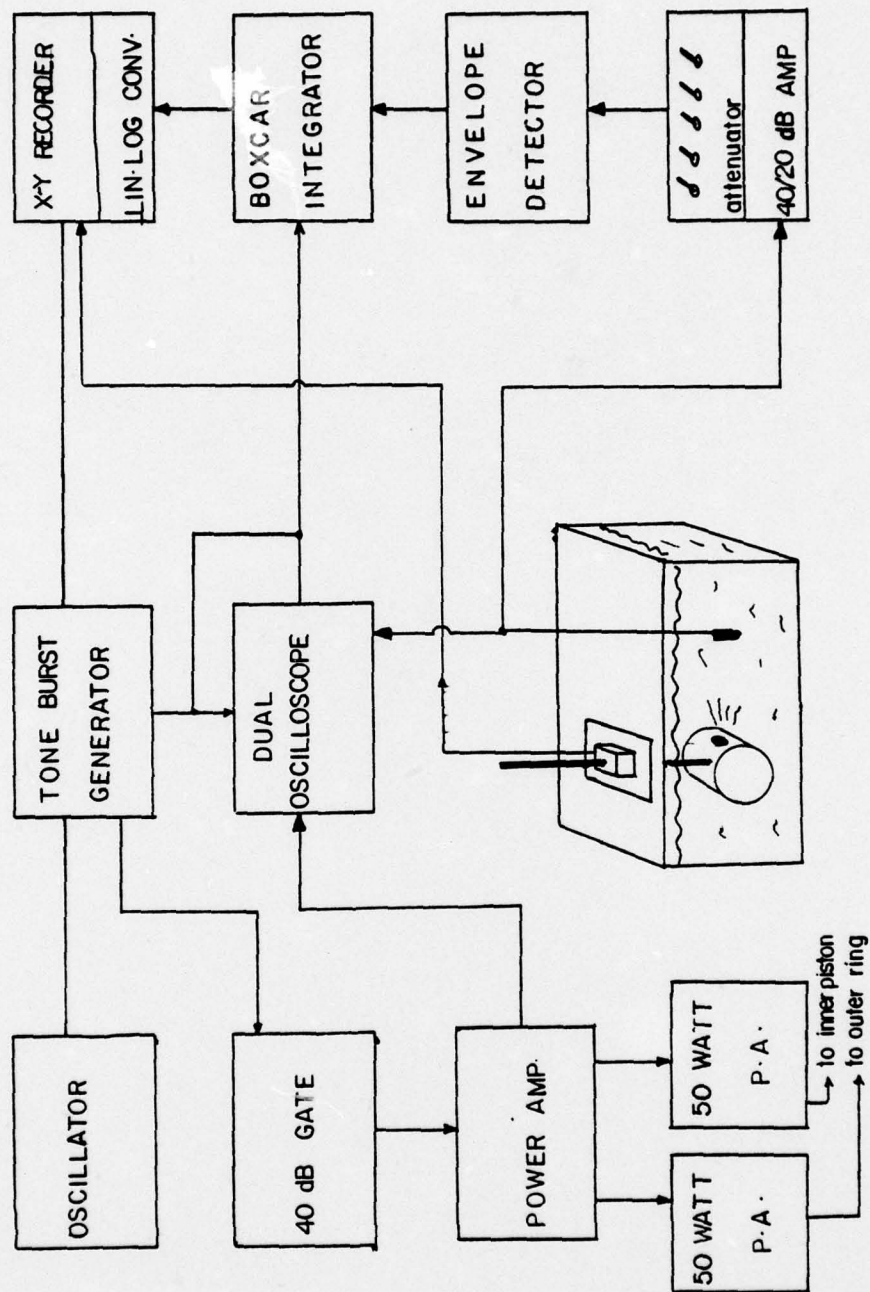
over the entire range.

FIG NO. 47 BEAM PATTERN MEASUREMENTS

INITIAL DISTRIBUTION LIST

No. Copies

1. Defense Documentation Center   2
   Cameron Station
   Alexandria, Virginia 23314

2. Director,Maritme Combat Systems   2
   National Defence Headquarters
   Ottawa,Ontario,K1A JK2
   Canada.

3. Library, Code 0212   2
   Naval Postgraduate School
   Monterey, California 93940

4. Department Chairman,Code 61   1
   Department of Physics and Chemistry
   Naval Postgraduate School
   Monterey,California 93940

5. Professor O.B. Wilson,Code 61 W1   5
   Department of Physics and Chemistry
   Naval Postgraduate School
   Monterey,California 93940

6. Department Library, Code 61   1
   Department of Physics and Chemistry
   Naval Postgraduate School
   Monterey,California 93940

7. Professor D.A. Stentz, Code 52 Sz   1
    Department of Electrical Engineering
    Naval Postgraduate School
    Monterey,California 93940

8. Dr. W. A. Middleton,Code 7002   1
    Naval Torpedo Station
    Keyport,Washington 98345

9. LCDR V.U. Auns   1
     Canadian Forces Maritime Warfare School
    C.F.B. Halifax
    Halifax,Nova Scotia,Canada

LIST OF REFERENCES

1. Shaw,A.H.P.,_Radiation Pattern Shaping of a Two Element,Concentric Ring Transducer Using Phase and Amplitude Shading_,M. S. Thesis, Naval Postgraduate School,Monterey,California,1975.

2. Green C. E.,_Polyalkylene Glycol as a Transducer Liquid_,Naval Undersea Center Report NUC-TP-390,May 1974.

3. _NAVORD 2814382_,Navord drawing 2814382-Output Specification Modified 28 Feb 1973.